



FFI-RAPPORT

17/16210

Nanosatellites in low earth orbits for satellite communications

—

Lars Erling Bråten
Andreas Nordmo Skauen
Abdikerim Yusuf

Nanosatellites in low earth orbits for satellite communications

Lars Erling Bråten
Andreas Nordmo Skauen
Abdikerim Yusuf

Norwegian Defence Research Establishment (FFI)

17 January 2018

Keywords

Nanosatellitter
Satellittkommunikasjon
Lav jordbane
Nordområdene

FFI-rapport

FFI-RAPPORT 17/16210

Prosjektnummer

1375

ISBN

P: 978-82-464-3022-5

E: 978-82-464-3023-2

Approved by

Richard Bjarne Olsen, *Research Manager*

Johnny Bardal, *Director*

Summary

In this study we consider the feasibility of utilising nanosatellites in low Earth orbits for continuous broadband communications in Norway and the Arctic. The objective was to investigate whether smaller and less costly satellites can offer high enough transfer capacity to be relevant in this context, and also to examine the maturity of nanosatellite technology. The findings are also compared to a previous study on microsatellites in highly elliptical orbits.

A coverage study was carried out to determine suitable orbits and the number of required satellites in the constellation. A Walker Star constellation with ten satellites in each of three orbital planes, having an altitude of 600 km and near polar orbits, provides continuous coverage. Orbital simulations have been utilised to investigate required solar panel and battery sizes. The power budget shows that it is possible to have 35 W available to the payload during the active period with a nanosatellite with deployable solar panels. This is sufficient for supporting an amplifier providing 10 W linear radio frequency power with 10 per cent duty cycle.

Dynamic link budgets have been developed to calculate expected communication capacity, assuming transparent communication payloads providing 5 W or 10 W signal power. Three different frequency bands have been considered, X, Ku and K/Ka (7.25–31 GHz). A solution with 10 W signal power can offer a system capacity of about 109 Mbit/s at X-band, 93 Mbit/s at Ku-band and finally about 52 Mbit/s at K/Ka-band. About half of the system capacity is obtained if reducing the signal power to 5 W. Capacity increase may be obtained by utilising more advanced technology, such as on board processing and satellite antenna spot beams, as well as by increasing the solar panel size, and thus available payload power.

Propulsion requirements have been considered based on launch opportunities, necessary velocity changes and available propulsion technology. The most promising solution is to utilise one launch per orbital plane, thus launching all the satellites in the same plane together. Ridesharing seems to be the most viable option, and over a period of a few years it should be possible to obtain close to the desired plane separation. If progress in the development of small satellite launchers continues, it may be possible in the next few years to combine dedicated launches with rideshare launches to ensure optimal orbits within a shorter timeframe. On-board propulsion is used for orbit maintenance. The lifetime velocity change requirement is within reach of available propulsions systems, assuming a mission lifetime of five to ten years.

The availability of rideshare launches to low Earth orbit is significantly higher than the previously studied highly elliptical orbit constellation with three microsatellites. The space radiation risk is also significantly lower compared to highly elliptical orbiting satellites. The study concludes that current nanosatellite technology is able to support relevant communication capacity for continuous Norwegian and Arctic coverage. We recommended carrying out a feasibility study, in cooperation with vendors, to determine if utilisation of small satellites is a cost-effective solution for a regional broadband system.

Sammendrag

I denne studien vurderes muligheten til å benytte nanosatellitter i lav jordbane for kontinuerlig bredbåndsdekning i Norge og Arktis. Formålet er å undersøke om mindre og rimeligere satellitter kan tilby høy nok overføringskapasitet til å være interessante i denne sammenhengen, og også å undersøke modenheten til nanosatellitteknologien. Det gjøres også en sammenligning med en tidligere studie som så på mikrosatellitter i høyelliptisk bane.

Dekningsberegninger har blitt utført for å identifisere en konstellasjon med passende baner og antall satellitter i hvert baneplan. En Walker Star-konstellasjon med ti satellitter i hvert av tre baneplan, med en høyde på 600 km og nær polare baner, gir kontinuerlig dekning. Banesimuleringer ble benyttet for å undersøke påkrevd størrelse på solceller og batterier. Effektbudsjettet viser at det er mulig å forbruke 35 W nyttelasteffekt i den aktive delen av banen med en nanosatlitt med utfoldbare solceller. Dette er tilstrekkelig for å forsyne et 10 W lineært radioeffekttrinn med ti prosent driftsperiode.

Forventet systemkapasitet har blitt beregnet ved hjelp av dynamiske linkbudsjetter ved å anta transparent kommunikasjonsnyttelast med 5 W og 10 W signaleffekt. Tre forskjellige frekvensbånd har blitt vurdert, X, Ku, og K/Ka (7.25–31 GHz). En løsning med 10 W uteffekt kan gi en systemkapasitet på om lag 109 Mbit/s i X-bånd, 93 Mbit/s i Ku-bånd og 52 Mbit/s i K/Ka-bånd. Kapasiteten reduseres til om lag det halve med en signaleffekt på 5 W. Kapasiteten kan økes ved å benytte mer avansert teknologi, som for eksempel ombordprosessering, satellittantennor med flekkstråler samt økt størrelse på solcellepaneler og derved økt nyttelasteffekt.

Krav til fremdrift er vurdert ut fra muligheter for oppskytning, behov for hastighetsendring og tilgjengelig fremdriftsteknologi. Den mest lovende løsningen er å benytte en oppskytning per baneplan, og dermed sende opp alle satellitter som skal til samme baneplan samtidig. Oppskytning som sekundær nyttelast synes gjennomførbart; i løpet av noen få år bør det være mulig å oppnå ønsket separasjon mellom baneplanene. Hvis fremgangen i utviklingen av små bæreraketter fortsetter som i dag, kan det om noen få år være mulig å benytte seg av en kombinasjon av dedikerte oppskytinger sammen med samkjøring. Dette kan være spesielt nyttig hvis det er få oppskytinger til de ønskede baneplanene, og det kan bidra til å sikre at optimale baner oppnås på kortere tid. Ombordfremdriftssystemet brukes for banevedlikehold. Hastighetsforandringen som er nødvendig for en levetid på fem til ti år, kan utføres ved hjelp av tilgjengelige fremdriftssystemer.

Oppskytinger som sekundær nyttelast er mer tilgjengelig til lav jordbane sammenlignet med den tidligere undersøkte konstellasjonen med tre mikrosatellitter i høyelliptisk bane. Strålingsmiljøet er vesentlig bedre i lav jordbane sammenlignet med høyelliptiske baner. Studien konkluderer med at nåværende teknologi for nanosatellitter understøtter relevant kommunikasjonskapasitet for kontinuerlig arktisk dekning. Vi anbefaler å utføre en mulighetsstudie, sammen med leverandører, for å fastslå om bruken av små satellitter er en kostnadseffektiv løsning for et regionalt bredbåndssystem.

Content

Summary	3
Sammendrag	4
Preface	8
1 Introduction	9
2 LEO constellation design	11
2.1 Constellation design	11
2.2 Coverage	12
2.2.1 Sensitivity analysis	14
2.3 Gateway assumptions	15
2.4 Radiation	16
3 Communication system	17
3.1 Feasibility of on board processing	17
3.2 Satellite antenna	17
3.2.1 Pointing accuracy and orbital altitude reduction	18
3.3 High power amplification	19
3.4 Payload and waveform assumptions	19
3.5 User terminal assumptions	20
4 Communications capacity	21
4.1 Calculated system capacity	22
5 On board power generation	27
5.1 Spacecraft	27
5.1.1 Communication system	27
5.1.2 Payload system	28
5.1.3 Attitude Determination and Control System (ADCS)	28
5.1.4 Computing system	29
5.1.5 Power system	29
5.1.6 Thermal system	29
5.1.7 Propulsion system	29

5.2	Solar power calculation	30
6	Constellation launch, deployment and maintenance	37
6.1	Perturbations	37
6.2	Orbital stationkeeping	38
6.3	Velocity change budget	39
6.4	Launch Opportunities	40
6.4.1	Dedicated Launch	40
6.4.2	Deployment Strategies	41
	6.4.2.1 Cluster launch of entire constellation	41
	6.4.2.2 Cluster launch per plane	41
6.4.3	Summary of launch strategies	42
6.5	On-board propulsion system	43
6.5.1	Potential propulsion systems	43
6.6	Summary launch and orbit maintenance	44
7	Summary	44
8	Comparison with highly elliptical orbit	45
8.1	Launch and propulsion	46
8.2	Spacecraft	46
8.3	System capacity and ground segment	46
9	Conclusions	48
	Appendices	49
A	Orbital manoeuvres, propulsion systems and launch opportunities - equations and background	49
A.1	Assumptions	49
A.2	Atmospheric drag	49
	A.2.1 Reduction in semi-major axis due to atmospheric drag	50
A.3	Earth's oblateness	51
A.4	Phasing manoeuvre	51
A.5	Deorbit	52
A.6	Cluster launch of entire constellation	53
	A.6.1 On-board propulsion system	53
	A.6.2 Nodal precession	53
	A.6.3 Manoeuvrable launch vehicle upper stage combined with a MPA	54
A.7	Propulsion system requirements	54

A.8 Launch	56
B Spacecraft mass and power budget	57
C Radiation	59
References	63

Preface

The work in this report is carried out under the FFI project number 1375 "MicroSatCom i Nord".

1 Introduction

The basic mission objective is to identify the feasibility of utilising nanosatellites in Low Earth Orbit (LEO) to provide real time, two-way broadband communication solutions for the High North. In a previous report, similar investigations were carried out for satellites in Highly Elliptical Orbits [1], showing the feasibility of utilising 2 - 3 microsattellites for providing in the order of 50 - 60 Mbit/s shared system capacity in the High North.

The coverage area considered include the Norwegian land and sea territory, economic zones and the Arctic search and rescue responsibility area. A map of the resulting area is shown in Figure 1.1. Note that this is a slightly extended area compared to the one used in the HEO study [1].

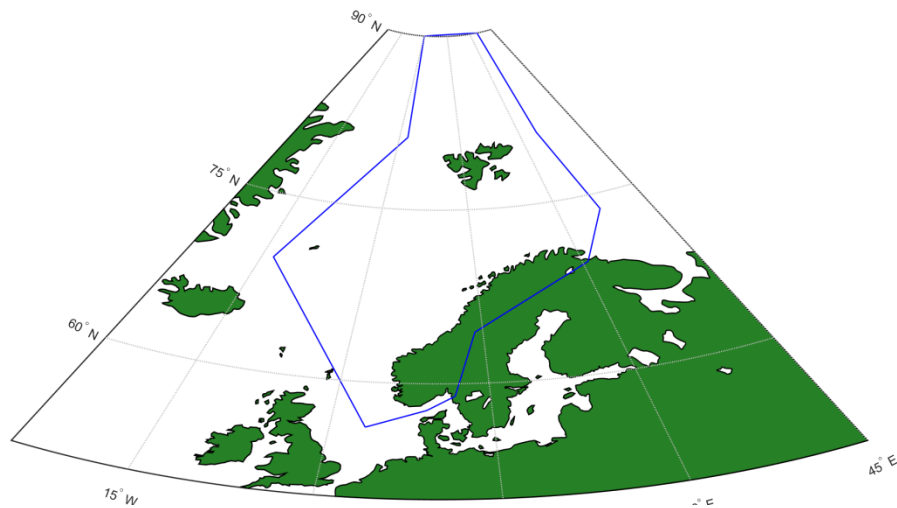


Figure 1.1 Coverage area.

The area is defined by the points in Table 1.1.

Latitude (deg.)	Longitude (deg.)
56.1	3.2
69.7	-13.4
81.2	2.1
90	0
81.0	34.3
73.7	37.0
69.5	30.8
64.4	14.1
58.9	11.5
57.7	8.8

Table 1.1 Coverage area.

We will perform the investigations for the governmental frequency bands, X- and K/Ka-band as well for the commercially available Ku-band, see Table 1.2.

Band	Uplink (GHz)	Downlink (GHz)
X	7.9 – 8.4	7.25 – 7.75
Ku	14.0 – 14.5	10.7 – 12.75
K/Ka	30.0 – 31.0	20.2 – 21.2

Table 1.2 Frequency bands communication services.

The primary purpose of investigating nanosatellites for two-way broadband communication is to see if they can become a cost effective alternative to more traditional communication satellites as they are less expensive and time consuming to develop. Secondly, technological advances have resulted in a miniaturisation of components, allowing for smaller satellites to perform to a level which previously could only have been achieved by larger satellites. Nanosatellites are also typically launched as secondary payloads, which significantly reduces launch costs, albeit with the disadvantages of being a secondary payload.

For this study, nanosatellites are considered to be satellites with a mass less than 10 kg. The authors have chosen a 3U CubeSat as a baseline platform in this study, although the concept can be scaled up to larger nanosatellites. The 3U platform has been selected due to it being a platform often used in industry for secondary payloads, which should make it easier to integrate on most launch vehicles. Finally, each subsystem has been designed for a 3U platform and the authors have considered all the subsystems together in terms of power, mass, volume and other parameters, such that they should fit together on a 3U. However, a detailed investigation of this has not been performed, and changes may occur at a later stage. The aim at this stage is to determine the feasibility of utilising nanosatellites, and detailed integration between the subsystems and with the satellite bus should be investigated at a later stage.

Payload linear radio frequency power is first assumed equal to either 5 or 10 W, corresponding roughly to the power generation potential of a 3U CubeSat satellite platform form factor with deployable solar cells. This starting point is based on the understanding that continuous coverage in the area of interest will require several tens of satellites, and we are targeting a relatively low cost system with limited regional broadband communications capacity in order of 50 to 60 Mbit/s. This is used as input to time dynamic link budgets and the system capacity is then derived. The feasibility of supporting the payload on a nanosatellite is then investigated. The satellite energy budget supporting the two options is estimated and orbit simulations utilised to find suitable solar cell area and battery size.

We are not investigating details regarding lifetime, however, propulsion requirements are derived for 5 and 10 years of system lifetime. For orbit maintenance, and also in some cases to get to the correct orbit, a propulsion system is required on the satellite. The state of the development of small satellites is described in for example [2]. Chemical propulsion systems are available for small satellites now.

The required pointing accuracy for communication satellites with regional or national coverage, foreseen to be within a few degrees, is within the current ability of 3-axis stabilised small satellites. There have been reported works on deployable antennas for communication, see for example [3]. Most of the reported results related to communications for small satellites are related to downlinking observations and performing control communication with the spacecraft bus and payload (TT&C). To the authors' knowledge, fewer results are available on payloads designed primary for a communication mission with relatively high transmission power combined with directive antennas and multiple simultaneous carriers.

The low Earth orbit constellation designed is discussed in Section 2 and the communication system in Section 3. The resulting system communications capacity is presented in Section 4, followed by on board power generation in Section 5. Launch and orbit maintenance is discussed in Section 6, followed by a summary in Section 7. The results are compared with a previously investigated highly elliptical orbit constellation in Section 8, followed by conclusions in Section 9.

2 LEO constellation design

Low Earth satellite orbits are usually circular orbits with a lower altitude limit of about 500 km due to atmospheric drag and an upper altitude limit of about 2000 km due to the lower Van Allen radiation belt. As the orbital altitude increases, the area visible from the satellite increases, resulting in a constellation with a lower number of satellites.

2.1 Constellation design

As the coverage area is located at relatively high latitudes, inclinations between 50 and 130 degrees, and specifically near polar orbits, are of interest. We have selected an example orbit with an altitude of 600 km and an inclination 87 degrees. This altitude is commonly reached or exceeded by LEO launchers for near polar orbits. As an example we also briefly investigate a similar constellation having an altitude of 1200 km to investigate the sensitivity to orbital height. The number of orbital planes should be minimised as the required velocity change, Δv , to change planes while in orbit is high, and normally one launch is required per plane, see Section 6.

We select to investigate an Iridium-like constellation with equal inclination for each plane, planes symmetrically distributed around Earth and the satellites evenly distributed within the plane. The satellites in neighbouring planes are staggered in phase to obtain improved coverage in a Walker Star design [4].

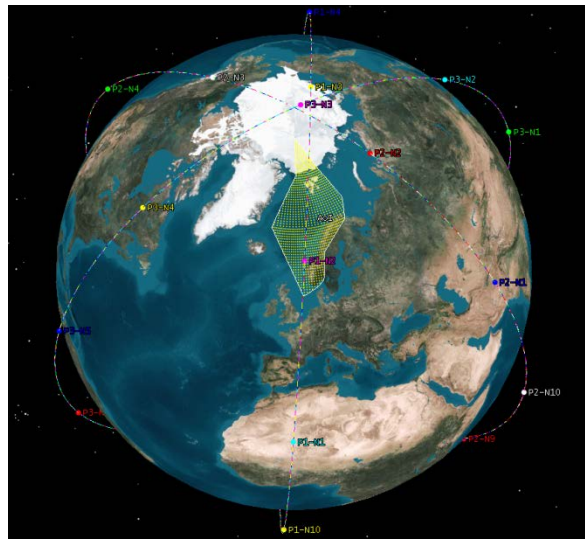


Figure 2.1 Constellation illustration.

We require continuous coverage of the area with at least one satellite visible above 5 degrees elevation angle. This applies simultaneously to terminals located within the coverage area and gateways.

2.2 Coverage

The coverage was simulated utilising System Tool Kit (STK) and a minimum elevation angle from the user terminal to the satellite of 5 degrees. The simulation time duration was 48 hours, sufficient for a reasonably accurate result although variations will still occur.

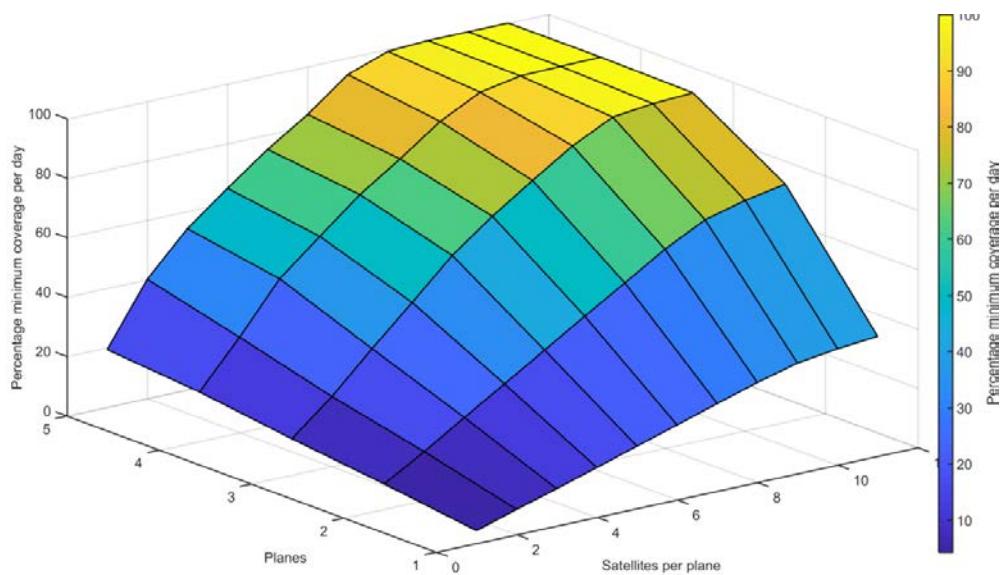


Figure 2.2 Satellite coverage as function of number of planes and satellites per plane.

The minimum number of planes required for continuous coverage is 4 planes with 11 satellites in each. However, 3 orbital planes with 10 satellites in each result in a daily minimum coverage of 98 % in the south and an average within the area of near 100 %, see also Figure 2.3 and Table 2.1.

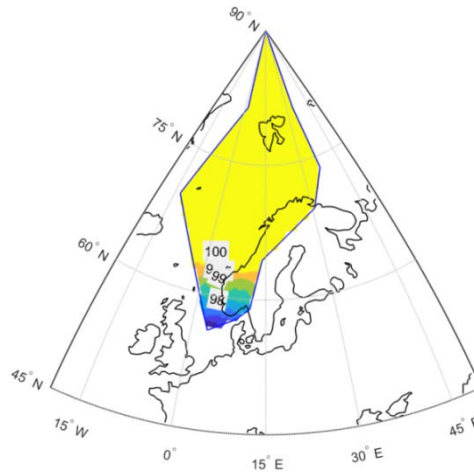


Figure 2.3 Percentage of time with satellite coverage within the area, 3 planes, 30 satellites.

The results in terms of daily minimum and average area coverage percentages are summarized in Table 2.1 for minimum elevation angles of ranging from 0 to 30 degrees.

Elevation (deg)	Planes	Satellites per plane	Min. coverage (%)	Avg. coverage (%)
0	3	11	100.0	100.0
0	3	8	98	100.0
0	2	13	95	99.9
5	4	11	100.0	100.0
5	3	11	99	100.0
5	3	10	98	100.0
5	3	9	97	99.9
5	3	8	90	98.9
10	4	18	100.0	100.0
10	4	12	98	99.9
10	3	20	95	99.8
20	7	28	100.0	100.0
20	6	19	98	99.9
20	6	17	95	99.6
30	10	25	98	99.8
30	9	24	95	99.4

Table 2.1 Minimum and average coverage as function of minimum elevation angle, 600 km altitude.

The number of satellites required increases significantly with increasing minimum elevation angle. A minimum required elevation angle of 20 degrees results in a constellation of $6 \times 19 = 114$ satellites having a minimum coverage (in the south of the coverage area) of 98 %. In comparison, a minimum elevation of 5 degrees requires a constellation with $3 \times 10 = 30$ satellites to obtain the same coverage percentage.

Note that a reduced area north of 70.1 degrees (not shown) results in a smaller satellite constellation with 2 planes with 10 satellites in each to obtain full coverage with a minimum elevation angle of 5 degrees.

Based on the availability of launches and their intended orbit characteristics (altitude, inclination), the actual constellation design can be optimised to ensure that reasonable coverage is obtained also in the southern parts of the coverage area. This also gives flexibility with respect to launch availability, compensating various orbit altitudes and inclinations with the number of satellites deployed. The most critical issue is probably to obtain a reasonably even inter plane spacing in terms of spreading the right ascension of the ascending node evenly around in the equator plane. One issue that could be investigated further is if the number of satellites can be reduced by employing irregular locations of the satellites in the plane (true anomaly), potentially obtaining improved regional coverage. With the required minimum elevation angle of 5 degrees, atmospheric propagation degradation effects are expected to be limited and assumed possible to mitigate with adaptive coding and modulation (ACM), even at Ka-band [5]. Maritime users are therefore expected to obtain high service availability, while landmobile and to some extent also aeronautical users in many cases will obtain reduced service availability mainly due to blockage effects and antenna pointing limitations. We select to continue studying the constellation with 30 satellites with 10 satellites in 3 orbital planes having an altitude of 600 km and an inclination of 87° .

2.2.1 Sensitivity analysis

Utilisation of sun synchronous orbits with inclination of 98 degrees at 600 km altitude will result in a slight reduction in coverage in the southern parts of the coverage area. With 30 satellites and a minimum elevation angle of 5 degrees, the minimum coverage time is reduced from initially 98 to 95 %. This could be considered an acceptable compromise enabling a wider variety of launch options. If required, this can be compensated for by increasing the total number of satellites from 30 to 48.

The effect of decreasing the orbit altitude due to orbit decay has a similar effect. At 550 km altitude for example, the coverage is reduced less than 1 % in the south of the coverage area if deploying 30 satellites with 87 degrees inclination.

A constellation having an altitude of 1200 km and the same inclination (87 degrees) would require a minimum of 2 planes with 11 satellites in each to obtain complete coverage given a required 5 degrees minimum elevation angle. If reducing the number of satellites in each plane from 11 to 7, the minimum coverage obtained in the southern part of the area is degraded slightly to 99.5 %. With 10 satellites in one single plane, a minimum coverage of 66 % and an

average coverage of 97.5 % are obtained. A single plane with 7 satellites results in a minimum coverage of 60 % and an average coverage of 94 %. This highlights the possibility of early operations while gradually deploying a constellation, and also the fact that fewer satellites is required if the orbital altitude is increased.

2.3 Gateway assumptions

At the gateway we assume utilisation of tracking parabolic antenna with a diameter of 3 m having an efficiency of 60 %. This is the same as assumed in [1], taking into account the goal of having a relatively low cost communications system.

We assume that no inter satellite links are utilised to simplify the satellite design. This implies that the satellite must simultaneously see users within the coverage area and one or more gateways to enable real time traffic.

The number of gateways required depends on the location of the gateway. To enable coverage in both the southern and northern parts of the coverage area we first investigate one single gateway located at Andøya. The coverage with one single gateway degrades the coverage area significantly, see Figure 2.4.

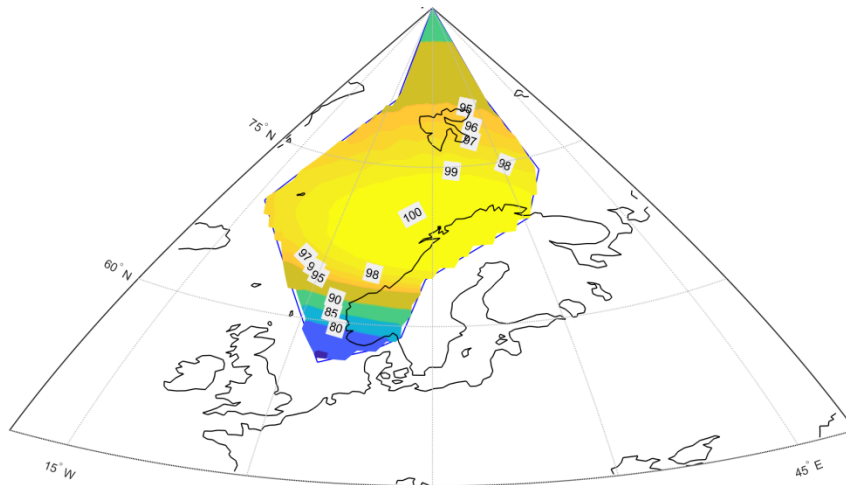


Figure 2.4 Gateway-satellite coverage, gateway located at Andøya.

The resulting coverage by locating gateways at Platåberget (Svalbard) and Bergen is shown in Figure 2.5.

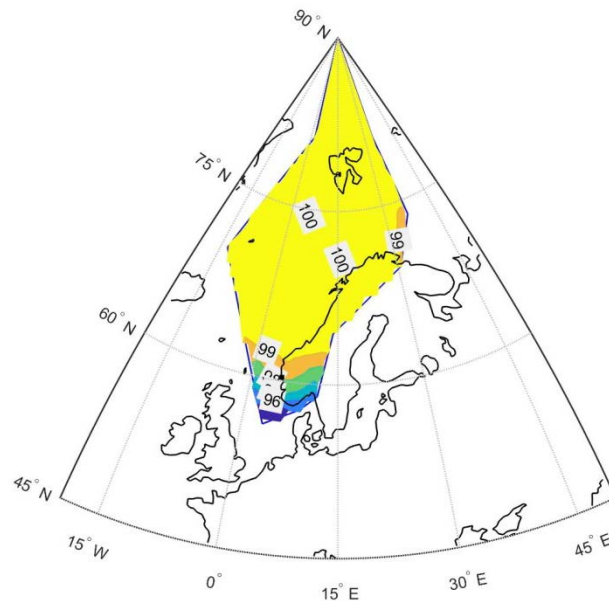


Figure 2.5 Gateway-satellite coverage, gateways located at Bergen and Platåberget, Svalbard.

The resulting coverage from utilising two gateways is considered satisfactory. The gateway in Bergen serves a maximum of two satellites simultaneously, while the one at Svalbard serves a maximum of 4 satellites.

2.4 Radiation

Space radiation for LEO-satellites has been discussed in a number of publications, including an internal study at FFI utilising Space Environment Information System (SPENVIS) [6]. A summary of expected radiation is given in Appendix C.

Experience with the AIS satellites indicates that radiation is not a major issue for LEO satellites if utilising industrial grade components and redundancy, if required.

3 Communication system

The payload system is discussed in this section, followed by requirements to power generation and energy storage in Section 4.

3.1 Feasibility of on board processing

As described in [1] several communication modules have been developed for downlinking high speed observation data. One recent example utilising the DVB-S2 standard together with a helix antenna operating at X-band to download observation data is given in [8]. The input to such transmit modules are digital data; hence a receiver demodulating the uplinks is required in addition with, or integrated with, the downlink module. Integration examples of a DVB-RCS2 receiver on a small satellite could be seen as the next logical step, however, to the authors' knowledge, this has not been shown yet. Although on board processing will reduce the required transmit power, the module's processing power consumption is critical for the current study of small LEO satellites. The availability of compact processing transceivers makes it somewhat unsure whether the technology is mature enough at the current stage. We therefore select to estimate performance in terms of capacity based on a traditional transparent transponder design only.

3.2 Satellite antenna

We have assumed a 600 km orbital altitude and a minimum terminal elevation of 5 degrees, resulting in an angular swath around the antenna boresight towards nadir of 2×66 degrees which should be covered by the satellite antenna. There are available isoflux antenna designs that compensate for the increased path loss with increasing off boresight angles, enabling almost constant ground flux density beneath the satellite. Different antenna designs have been reported; examples include helix [9], concentric rings [10], choke horn [11], patch and finally a compact design for nanosatellites [12]. In Figure 3.1 the theoretical isoflux satellite antenna gain is shown based on inverted free space loss at X-band together with the measured antenna gains for helix [8], compact [12] and an example patch.

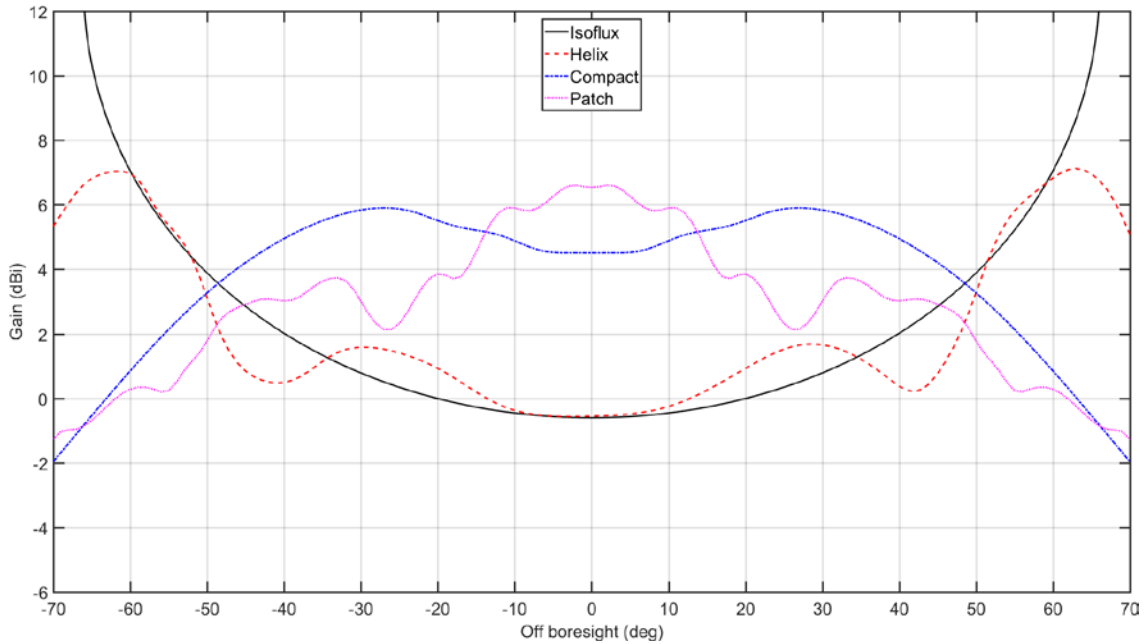


Figure 3.1 Ideal isoflux satellite antenna gain, X-band.

The helix antenna best resembles the isoflux antenna pattern. The physical design of the compact and patch antennas may enable easier integration on a small satellite, however, deploying the helix when in orbit is possible.

We will assume that it is possible to implement compact low weight near isoflux antennas at the frequency bands investigated. Although satellite antennas with multiple spot beams are available, none were identified for use on small satellites. However, at Ka-band, traditional designs might become compact enough to enable utilisation on nano- and microsatellites. No attitude optimisation has been accounted for in the study, and the satellite antenna is pointing towards nadir when serving the coverage area. In the following dynamic power link budget calculation we utilise the helix antenna pattern.

3.2.1 Pointing accuracy and orbital altitude reduction

With the low gain satellite antennas discussed in the previous section the pointing accuracy required from an attitude control system is modest. We will initially assume a nadir accuracy of ± 2 degrees corresponding roughly to 1 dB change in the antenna gain at the end-of-coverage. It is expected that the effect of decreasing the accuracy to ± 3 degrees, or even ± 5 degrees, is modest on the link budget results, depending somewhat on the selected antenna pattern.

As will be discussed in Section 6.1, one of the major orbital perturbation forces is atmospheric drag, gradually decreasing the satellites orbital altitude if a propulsion system is not used to counteract the drag. Seen from a communications perspective, a gradually decreasing orbital altitude over a system lifetime of for example 5 to 10 years might not pose a problem as long as the satellite phasing in the orbital planes is maintained. As an example, assume that the 3-plane, 30-satellite constellation orbital altitude is reduced from 600 to 550 km, maintaining the

required minimum elevation angle of 5 degrees within the national coverage area. This results in a minimum coverage of 97.6 % and an average of 99.91 %. Compared to the results in Table 2.1, with minimum coverage of 98.7 % and average of 99.96 %, the reduction in coverage is not considered significant. The constellation communication performance is considered relatively insensitive to satellite altitude decrease over time.

3.3 High power amplification

For the currently investigated nanosatellites we are looking at saturation power in the range of 5 to 10 Watt (W) and linear operation for multicarrier transmission.

The dominating power consumption part in a communication payload is normally the high power amplifier. The high power amplification technology utilised today is mainly Travelling Wave Tube Amplifiers (TWTAs) above C-band. However, Solid State Power Amplifiers (SSPAs) is utilised for terminals up to at least Ka-band if requirements on power efficiency is moderate. When compared to TWTAs, SSPAs usually has lower mass, lower efficiency and avoids the need for the TWTs high voltage supply. At higher power levels, the power efficiency of TWTAs is often better than SSPAs. High Power Amplifier (HPA) power efficiency is assumed to be about 60 % for TWTAs including the power supply [13].

The SSPAs tend to have efficiencies between 12 and 25 %, the higher end typically for space qualified products. For a recently developed 15 W X-band SSPA, an efficiency of 34 % was obtained [14]. There is a development towards gallium arsenide (GaN) amplifiers with power levels exceeding 100 W, achievable now at X- and Ku-bands [15]. A 17 W X-band SSPA from General Dynamics was developed for the Mars Exploration Rover mission [16].

If the power budget is tight, one alternative is to perform on-board demodulation of the received signals from the terminals and gateway and transmit a single carrier down with a minimum of back-off to reduce distortion due to intermodulation. The uplink may then utilise standard multiple access techniques such as frequency division multiple access (FDMA) or multi-frequency time division multiple access (MF-TDMA), with time division multiplex on the downlink.

3.4 Payload and waveform assumptions

The satellite system noise temperature is assumed equal to 410 K for all 3 considered frequency bands. The antenna temperature is conservatively set to 290 K, a LNA noise figure of 1.5 dB, and a receive/transmit waveguide loss of 1 dB. The satellite gain (excluding antennas) is set to 115 dB, resulting in retransmitted noise power of about 0.07 W (1.3 % of 5 W) if the transponder bandwidth is 38.4 MHz. During the simulations it is assumed that active satellites operate at different frequency ranges to avoid interference.

Also the waveform performance is of importance. We have assumed a minimum E_b/N_0 of 3 dB, QPSK modulation and root-raised cosine filtering having a roll-off of 20 %. A guard band of additional 10 % is allocated between carriers to reduce the level of adjacent carrier interference.

We will utilise the same satellite antenna gain beam width for both up- and downlink, although the frequency ranges differ, especially at Ka-band.

We have assumed that 5 or 10 W of linear signal power is available from the satellite HPA to enable a nano-satellite design. The actual power available for, and consumed by, the payload is scalable in this stage of the design process. With an efficiency of 33 %, this translates to a DC power consumption of 15 or 30 W. Allowing some power to other payload components, such as mixers and LNAs results in a total power consumption in the order of 18-20 W for the low power version and 33-35 W for the high power variant. The duty cycle of the payloads is on average 9.5 % of time, and an assumption of 10 % duty cycle will be utilised when developing the power consumption budget.

3.5 User terminal assumptions

Utilisation of low gain user terminal antennas similar to the previously discussed isoflux antennas for the satellites is clearly of interest to reduce user terminal complexity and costs. Although not shown, low gain antennas on both the satellites and user terminals do not provide sufficient power to close the link budgets in the case of broadband communications.

With parabolic tracking antennas, each terminal would require two antennas to avoid signal loss while switching to another satellite. Adaptive (phased array) antennas may obtain good performance if the physical layout resembles a hemisphere [17]. Similar to the solution with two tracking antennas, the cost, weight and spatial requirements may be a challenge for low cost and mobile terminals. Flat panel adaptive antennas, without mechanical steering or utilisation of more than one panel, suffer from scan loss, and may be a good alternative only if designing the system for a higher elevation angle. As seen in Table 2.1, the required number of satellites increases significantly with the minimum elevation angle, thus flat panels are not considered further here. They might however, become of interest for HEO systems with satellites high above the local horizon.

Maritime vessels often have two tracking antennas installed to enable diversity and thereby avoiding link interrupts due to ship structures blocking the signal to/from the satellite.

Location of the antennas on airplanes, and the number and sizes of antennas employed, often implies a minimum required elevation angle in order of 20 to 30 degrees. This is due to antenna design and location on the airplane, scan loss (for adaptive antennas) as well as the flight pattern in terms of deviation from the horizontal plane during turns and altitude changes. The considered LEO constellation would consequently not provide continuous coverage and interruptions, especially in the southern parts of the coverage area, will occur.

Vehicular antennas for land mobile users can track (single) LEO satellites down towards the local horizon. The actual elevation angle required to obtain line-of-sight towards the satellites varies with the environment, including terrain shape, man-made obstacles such as houses and not least the vegetation in form of trees [18]. With a single antenna, interrupts during satellite handover will occur regularly.

Similarly to the dimensioning example in [1] we will employ a parabolic user terminal antenna with diameter of 0.8 m, an efficiency of 60 % and the assumptions in Table 3.1. This antenna size is considered representative for small maritime vessels; land mobile and aeronautical antennas may be smaller.

The solid state High Power Amplifier (HPA) or Block Up converter (BUC) saturation output power will vary with terminal size and bit rate requirements. We have assumed maximum linear operational power in the order of 10 W for a single channel per carrier (SCPC) link. A summary of the terminal assumptions are given in Table 3.1, where the sensitivity of the receiver is represented by G/T and the transmitter characterised in terms of Effective Isotropic Radiated Power (EIRP).

Frequency band	X	Ku	Ka
Max transmit power (W)	10	10	10
Antenna diameter (cm)	80	80	80
Transmit gain (dBi)	35	39	46
Max EIRP (dBW)	43	47	55
G/T (dB/K clear sky)	10	14	18

Table 3.1 Assumed terminal gain, EIRP and G/T .

The receiver Low Noise Block (LNB) down converter is assumed to have a noise factor of 1 dB. The terminal antenna pointing loss is assumed equal to 1. The ohmic losses before the LNB and after the HPA are both assumed equal to 1 dB. Similar values are utilised for all three bands, although it is noted that for example waveguide loss increase with frequency.

4 Communications capacity

System capacity has been estimated by distributing a number of users randomly within the coverage area and calculating the required maximum satellite HPA power. The number of users was calculated ensuring the maximum of 5 or 10 W satellite signal power was not exceeded any time. The gaseous attenuation, rain and cloud attenuations were calculated according to ITU-R

recommendation [19] with 95 % required availability, taking into account the terminal location and dynamically changing elevation angle. Significant excess attenuation is observed especially at the Ka-band uplink when the elevation angle is low. The gateway and terminal noise temperatures are calculated following the procedure in the same recommendation, based on gas, cloud and rain attenuation. Ground temperature is included taking into account an empirical elevation angle dependence. Automatic uplink power control was applied to both gateways and terminals to minimise the transmitted power obtaining the required signal-to-noise ratio. We assume ACM is utilised to maintain service availability during unfavourable conditions with somewhat lower information bitrates.

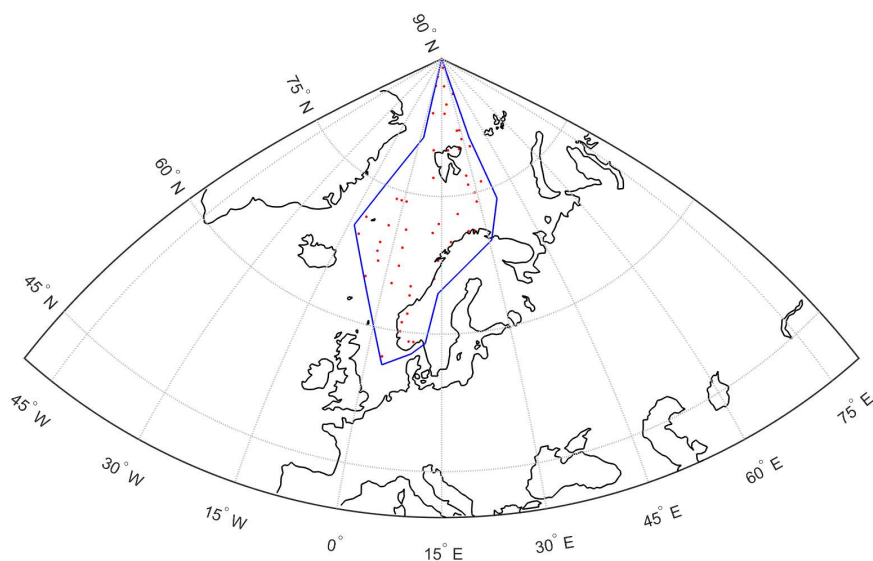


Figure 4.1 Example of 58 user locations (red dots) randomly located within the coverage area.

The modulation assumed is QPSK, with a Forward Error Correction (FEC) rate of $\frac{1}{2}$, resulting in a symbol rate equal to the information bit rate. The required bit energy to noise floor, E_b/N_0 , is assumed equal to 3 dB, corresponding to a carrier power to noise floor, C/N_0 , of 63 dBHz for an information bit rate of 1024 kbit/s. A minimum elevation angle of 5 degrees is imposed for both the gateway and the user terminal to avoid unrealistically pessimistic channel degradation assumptions and to increase the probability of line-of-sight without obstacles (for example terrain and vegetation) towards the satellite. The satellite is assumed steered to point the fixed antenna towards Earth's centre (nadir).

4.1 Calculated system capacity

The system capacity was estimated utilising the same terminal and gateway locations for 3 frequency bands: X, Ku and Ka.

The number of terminals deployed was increased to obtain service availability of about 95 %. Outages can occur due to a number of reasons, for example due to transmit power limits being exceeded, too low elevation angles etc. For most systems the availability can be increased by utilising waveform adaption in terms of ACM or transfer rate reduction, hence the somewhat low service availability required for the simplified simulation results reported here. The numerical values utilised for determining outage are summarised in the list below:

- Terminal elevation angle less than 5 degrees
- Terminal transmit power exceeds 10 W
- Terminal received total E_b/N_0 less than 2.99 dB
- Gateway elevation angle less than 5 degrees
- Gateway aggregated transmit power exceeds 500 W
- Gateway received total E_b/N_0 less than 2.99 dB
- Satellite transmit power exceeds 5/10 W

Dynamic power link budgets were developed for calculation of received power as function of geometry and antenna gains. In cases where the satellite transmit power exceeds the limit, the most demanding forward downlink is dropped in both the forward and return directions. This is repeated until the required aggregated power to close the links is below the limit.

Power balancing between satellites has not been implemented, the satellite nearest the user terminal is selected to be the serving satellite.

The estimated simultaneous system capacity at X-band for 33 terminals operating symmetrical 1024 kbit/s with an availability of 95 % was on average 64.5 Mbit/s (minimum 41.0 Mbit/s) of the desired maximum 67.6 Mbit/s. The variations in system capacity with time are depicted in Figure 4.2 and the cumulative distribution of throughput in Figure 4.3.

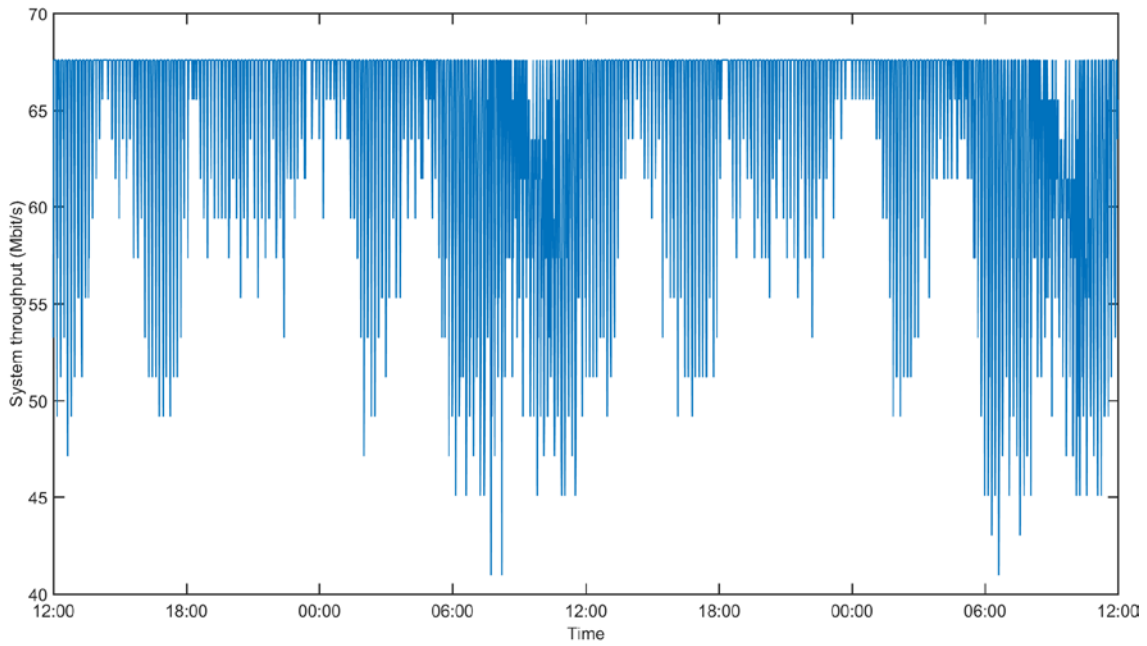


Figure 4.2 System throughput as function of time at X-band with 33 terminals.

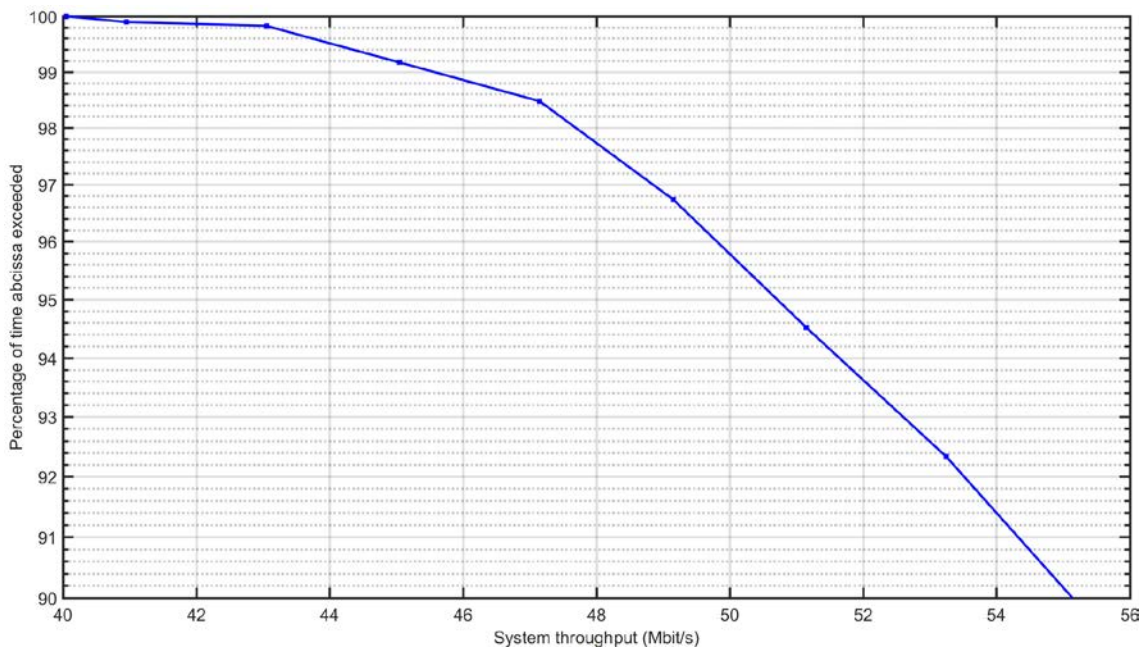


Figure 4.3 Complementary cumulative distribution of system throughput at X-band with 33 terminals.

The capacity exceeded 50.7 Mbit/s for 95 % of the time, which is near the theoretical maximum throughput given the bit rates and number of terminals applied.

The maximum satellite signal power was 5 W, with an average of 0.23 W and a mean duty cycle of 9.3 %. The maximum user terminal transmit power was 10 W and the maximum gateway power 12.5 W. The complementary cumulative distribution of satellite power is depicted in Figure 4.4.

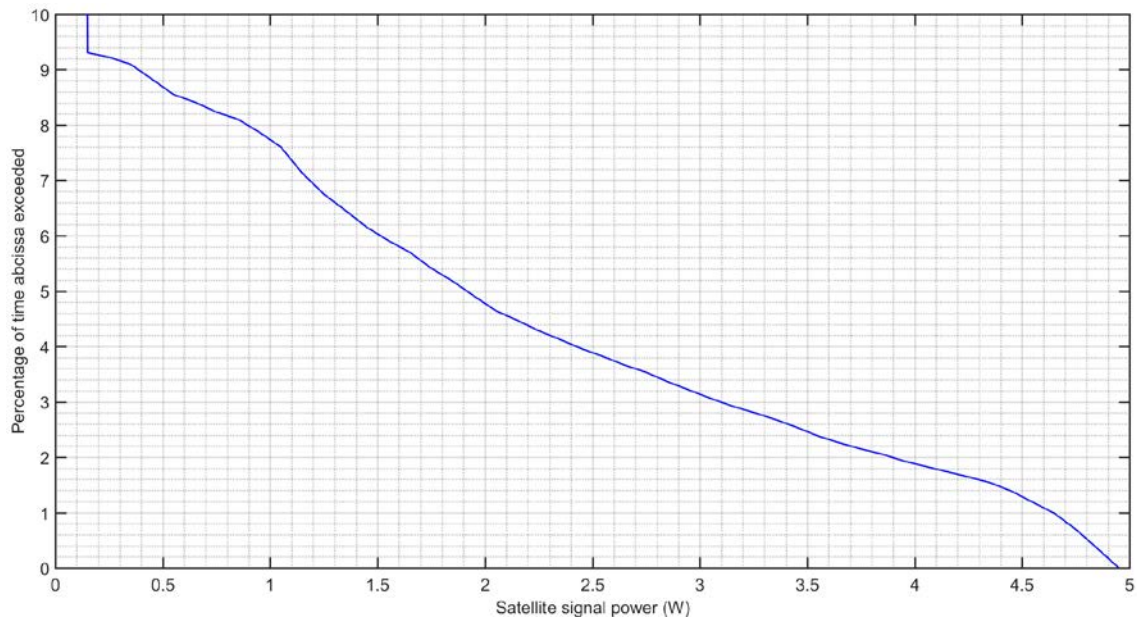


Figure 4.4 Cumulative distribution of satellite transmission power at X-band with 33 terminals.

Satellite signal power exceeds 4 W for 1.9 % of time and 3 W for 3.1 % of time. The discontinuity observed for low power is caused by noise power re-transmitted from the satellite also in cases when no carriers are transmitted via the satellite relay.

Average uplink excess attenuation (gas, rain and cloud calculated for 5 % of time) was 0.21 dB for the gateways and 0.22 dB for the terminals, with a total average of 0.22 dB. Terminal total availability was 95.4 % of time, mainly limited by the available satellite power causing 3.9 % of the outage time.

Similar results were obtained and summarised in Table 4.1 for the Ku- and Ka-bands. At Ka-band the forward downlinks (to the terminals) are challenging to close due to the necessity of higher satellite power due to increased excess attenuation. The return uplinks are challenging to close as well due to the limitation of 10 W transmit terminal power. The information bit rate at Ka-band to/from the terminals is therefore reduced from 1024 to 128 kbit/s.

Band	Terminals	Cap _{95%} (Mbit/s)	A _{tot} (%)	O _{elev} (%)	O _{SA-tx} (%)	O _{UT-tx} (%)	UL _{excess loss} (dB)
<i>5 W satellite transmit power</i>							
X	33	50.7	95.4	0.4	3.9	0.2	0.2
Ku	27	42.2	95.5	0.4	2.8	1.3	0.5
Ka	122	24.8	95.2	0.3	1.2	3.3	2.0
<i>10 W satellite transmit power</i>							
X	69	109.1	95.3	0.4	4.1	0.2	0.2
Ku	58	92.8	95.2	0.4	3.2	1.3	0.5
Ka	255	51.8	95.1	0.3	3.5	1.1	1.9

Table 4.1 Estimated system capacity at X-, Ku- and Ka-band. A_{tot} : total availability, O_{SA-tx} : outage due to satellite power limitation, O_{UT-tx} : outage due to user terminal power limitation, $UL_{excess loss}$: uplink gas, rain and cloud attenuation.

The highest system capacity is obtained at X-band, with about 51 Mbit/s given a maximum satellite transmit power of 5 W. At Ku-band it is reduced to about 42 Mbit/s while the capacity at Ka-band is 25 Mbit/s. If increasing the satellite transmit power to 10 W, the X-band capacity increases to 109 Mbit/s while at Ku- and Ka-band the resulting system capacity becomes 93 and 52 Mbit/s respectively.

One may want to consider the possibility of utilising satellite spot beams with higher antenna gain at Ka-band to improve the system capacity and to enable higher transmission rates. Although solutions for small satellites to the author's knowledge are not currently available, the short wavelength might enable either a multi beam solution or a single hopping beam. By utilising a more advanced attitude control it might also be possible to reduce the antenna beam width, still obtaining the coverage resulting from an isoflux antenna by taking into account the actual location of the users.

5 On board power generation

In this section the power consumption is estimated for a nanosatellite with attitude control for antenna and solar cell pointing. The power generated is estimated based on the solar cells located on the satellite body as well as form a deployable panel. Orbital simulations are utilised to calculate generated power over time for different orbital planes and battery sizes supporting the total power consumption is estimated.

5.1 Spacecraft

In general, in addition to the mechanical structure, a spacecraft broadly consists of:

1. Communication system
2. Payload system
3. Attitude Determination and Control System (ADCS)
4. Computing system
5. Power system
6. Thermal system
7. Propulsion system (if applicable)

Each of these systems should be optimized for the mission objective (broadband communication service in the High North), operations concept (analogue/digital transponder) and payload requirements (power consumption, pointing requirements, temperature requirements etc.). For low-cost missions, some optimization can be traded for cost-reduction.

Based on the previous sections on mission objective and the concept of operations an outline of the spacecraft systems can be sketched in terms of required and available technology. The outline will be used later in Section 5.2 to estimate the possible power generation on a satellite platform in low Earth orbit.

5.1.1 Communication system

In general, the communication system must be designed to support the operations concept and the payload data up- and downlink. In this case the payload is a communications payload that does not require additional downlink capacity beyond nominal housekeeping telemetry.

While the payload is a communications payload, it is not prudent to rely on the high power communications payload only for communications. In case the satellite enters recovery mode (or even during commissioning), where power generation or attitude control is insufficient for

the high power communications payload operations, a way of communicating with the satellite is still required.

For command uplink and telemetry downlink, including payload housekeeping telemetry, a low power UHF band transceiver is considered suitable for such a nanosatellite mission as discussed herein. The power consumption, not the frequency, of the transceiver is the important parameter so if alternative higher frequency transceivers are identified these can also be used.

5.1.2 Payload system

The proposed payload system was discussed in Section 3.

5.1.3 Attitude Determination and Control System (ADCS)

The ADCS must be designed to support the operations concept and attitude determination and control requirement imposed by the payload.

The operations concept to keep the spacecraft fixed communication payload antenna pointed towards nadir, while keeping one particular side towards the sun as much as possible, requires three axis control of the spacecraft. Small satellites typically use reaction wheels as actuators for precision three axis control. Other alternatives exist, like control moment gyroscopes if large torque is required, or pure magnetorquer control system if the control requirements are low. For the proposed concepts, the torque and control requirements best match the use of reaction wheels.

The attitude knowledge and control requirements in order to point the antenna main lobe towards nadir are modest, with a required accuracy of +/- 2 to 5 degrees for the proposed payload antennas.

Additional sensors and actuators, such as sun sensors, accelerometers, magnetometer and magnetorquers or propulsion units, are required for momentum dumping and coarse attitude determination and control during sun-pointing power generation mode, recovery mode or other low-power modes. For low Earth orbits magnetorquers provide an efficient means for momentum dumping and propulsion units are not required for this purpose. Since propulsion is necessary for the required constellation maintenance, propulsion units for momentum dumping could be explored in a detailed design phase

For orbit determination GPS signals provides an accurate method, however, it requires more power than one is believed willing to accept for this mission. If on-board orbit propagation based on uploaded orbit state parameters (e.g. two-line elements) is insufficient, an alternative is ranging techniques performed at/by the gateway station. However, on-orbit propagation based on uploaded state parameters is believed to be sufficient for this mission.

5.1.4 Computing system

The computing system is responsible for command and data handling, monitoring the overall status of the satellite bus and operating the ADCS.

5.1.5 Power system

The power system must be able to support both the peak power and total energy requirement of the spacecraft operations implied by the operations concept. The total energy requirement will drive the sizing of the solar panels, while the peak power requirement and/or eclipse operations, will drive the sizing of the batteries required. High efficiency (28 %) solar cells and high energy density batteries (Li-Ion 150 W-hrs/kg) are commonly used in modern small satellites and is proposed here also.

The power system required for the different platforms are discussed in more detail later in Section 5.2.

5.1.6 Thermal system

The electrical components that make up the aforementioned subsystems are designed to operate within a specified temperature range. In the vacuum of space heat exchange is only via radiation (and conduction internally), and thermal management can be difficult since the side facing the sun can get very hot, while the sides facing into deep space can get very cold. In addition, most LEO orbits will have periods of eclipse, in which the Earth is blocking the view of the sun from the satellite perspective. In eclipse, the satellite must rely on internal heating alone to not exceed the minimum temperature limits of the satellite components. On the other hand, while in the sun, the combination of sun heating and satellite internal heating must not exceed the maximum temperature limit of the satellite components. Typical thermal management of small satellites is achieved passively through manipulating the satellite emittance and albedo by using different colour tape or paints on the satellite body. In addition, the batteries typically require heaters, since batteries do not operate well when cold and the satellite itself may not provide enough internal heating in recovery modes where most of the systems are switched off.

Particular to the concepts discussed in this report is the relatively high power communications payload that will create a significant amount of heat that the satellite must get rid of. Thermal management considerations are outside the scope of this study, but is an area that warrants further investigation.

5.1.7 Propulsion system

The propulsion system must be scaled to support any orbital changes, formation flying and station keeping that the operational concept requires. For the proposed concept, both chemical and electric alternatives are found viable in Section 6.

The required technologies discussed yields an implied starting point for the power and mass budgets of Appendix B, before sizing the power, payload and propulsion system, and are estimated in the current report to be within the scope of a small satellite mission.

5.2 Solar power calculation

A 3U platform was selected as the baseline for the power calculations in this report. Three different configurations were investigated with respect to the solar panel size and the resulting power generation.

1. Standard 3U with solar cells on every face apart from the payload antenna face.
2. 3U platform as in 1. with two unfolding wings with solar cells in addition
3. 3U platform as in 1. with four unfolding wings with solar cells in addition

28% solar cell efficiency is assumed for all calculations. Furthermore, the results are presented as end-of-life results, assuming a 70 % degradation of the solar panels, 80 % efficiency from solar panel to load and an average power flux from the sun of 1361 W/m^2 [26], but no reflected sunlight from Earth. It is also assumed that the effective solar panel area of each face is 60 % to accommodate sensors, mechanisms, structural elements etc. on the theoretically available max 10 cm x 30 cm main body and per wing area [20].

A power generation analysis was performed using STK attitude control and sun incidence calculations for 600 km altitude LEO orbits for the three platforms. The analysis assumed that the solar panels were fixed with the satellite body, i.e. the panels did not have a mechanism to rotate independently from the satellite body. The attitude control mode implemented was one in which the Z-axis, assumed to be the payload antenna axis, is pointed towards nadir while the ground to satellite elevation angle is greater than 5 degrees, while at the same time trying to align the X-axis with the sun. When the elevation angle requirement is no longer satisfied, the X-axis is aligned with the sun angle only, see Table 5.1.

Access to area of interest	Primary attitude requirement	Secondary attitude requirement
Yes	Z-axis aligned with the vector towards nadir	X-axis aligned with the vector towards the sun
No	X-axis aligned with the vector towards the sun	N/A

Table 5.1 Assumed satellite attitude control strategy.

Furthermore, the amount of power assumed used by the satellite platform to perform the pointing and operate other support functions for the payload is summarized in Table 5.2 (see Appendix B for details). Without a detailed design, these values are considered moderately conservative. Examples can be found of 3U platforms using considerably less power, but equally examples can be found that use more [20][22].

Access to area of interest	Satellite platform power use
Yes	6.8 W
No	4.2 W

Table 5.2 Assumed satellite platform power use.

The sum of all these assumptions can be considered to be a conservative approach.

Figure 5.1 - Figure 5.3 show the yearly power surplus as a function of the right ascension of the ascending node (RAAN), i.e. the orbital plane, available for a payload on the three 3U platform alternatives respectively. The upper plot shows the minimum orbit power surplus, i.e. the minimum amount of power surplus of any orbits in the year. The middle plot shows the maximum amount of power surplus, while the lower plot shows the orbit average power surplus. A variation with RAAN is clearly visible and should be accounted for in selecting the orbital parameters of the system and in designing the satellites. The curves are virtually identical for the three platform alternatives, and will be identical in shape for all types of platforms with the attitude control strategy of Table 5.1 and platform power consumption of Table 5.2, but the power surplus values (y-axis) varies with the solar panel size and geometry.

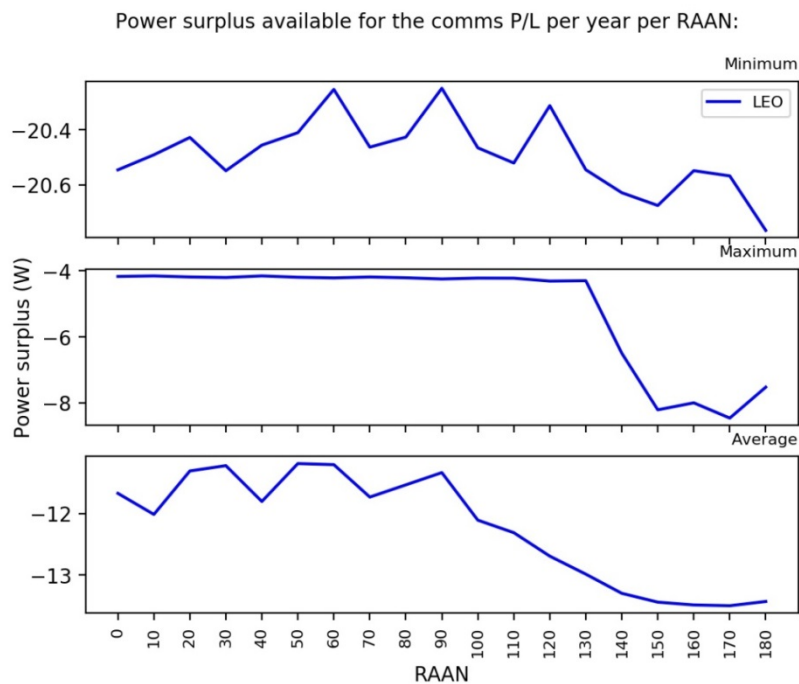


Figure 5.1 Minimum, maximum and average power surplus available per orbit per year per RAAN for a 3U platform body mounted solar panels only.

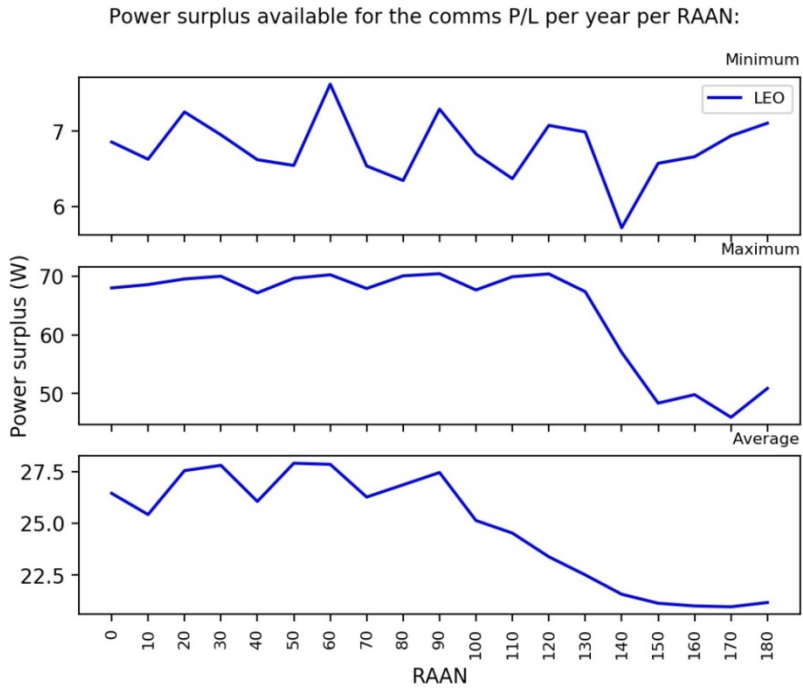


Figure 5.2 Minimum, maximum and average power surplus available per orbit per year per RAAN for a 3U platform with two unfolding wings.

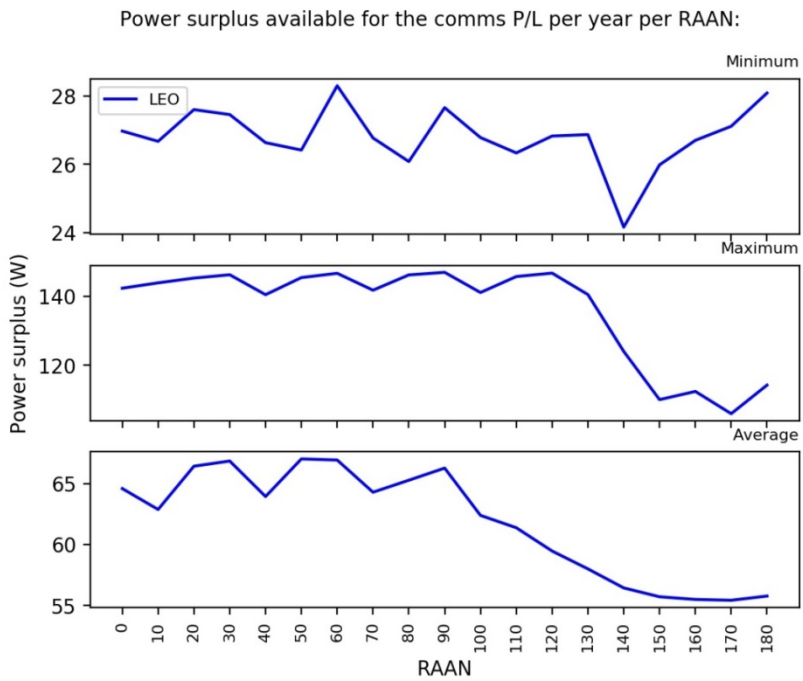


Figure 5.3 Minimum, maximum and average power surplus available per orbit per year per RAAN for a 3U platform with four unfolding wings.

Figure 5.4 shows the monthly variation in the power surplus for a particular RAAN for a 3U platform with two unfolding solar panel wings. Again, the curves will be identical for all platforms using the same attitude control strategy and bus power consumption, but the amplitude is determined by the available solar cell area and geometry. The blue curve shows the minimum-, the red curve the maximum- and the green curve shows the average orbit power surplus.

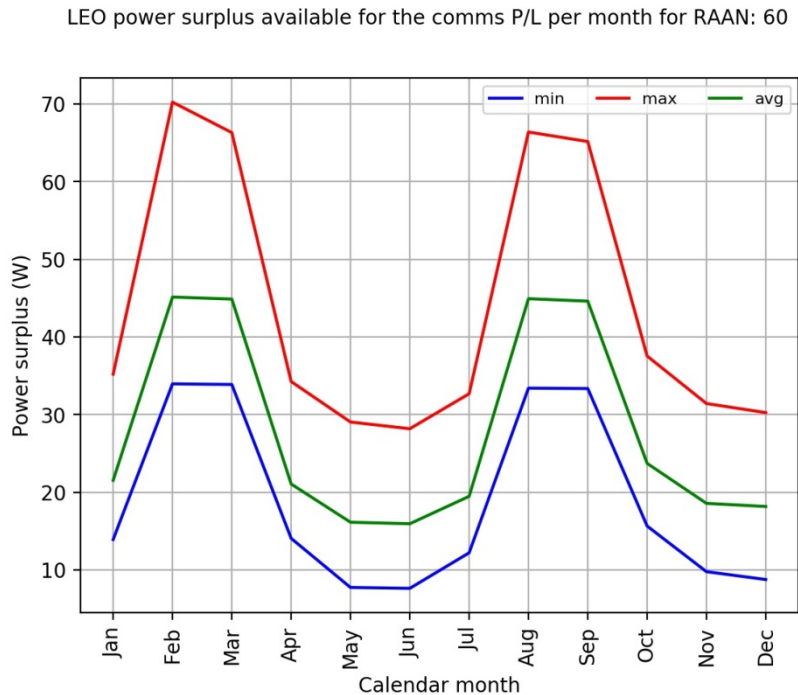


Figure 5.4 Minimum, maximum and average power surplus available per orbit per month for a 60° RAAN for a 3U platform with two unfolding solar panel wings.

The power surplus is calculated from the energy that can be collected by the satellite, less the amount of energy used by the platform, without payload operations, during an orbit as previously detailed in [1]. By assuming that all this surplus energy is used only when the payload is active yields the power surplus available for the payload.

It can be seen that the 3U platform with no unfolding solar wings cannot even sustain the platform power consumption estimated, let alone a transponder. The 3U with two unfolding wings can nearly sustain a 10 W transponder payload, but not quite, while adding another two solar wings typically allows at least 25 W transponder payload power consumption.

However, such a definition of power surplus available for the payload assumes there is enough battery on board the satellite to store, and use, all the surplus energy.

Assuming a maximum 25 % depth of discharge, and 150 Whr/kg battery energy density with full redundancy it is possible to estimate the battery pack required to support different communication payload power consumptions. Figure 5.5 shows the required average and maximum battery pack requirement to support 5 W to 25 W payload power consumption for the 3U alternative with four unfolding wings. The figures show that a maximum battery pack between 40 Whr and 90 Whr is required. Note that not all RAAN selections can support a 25 W payload regardless of the battery size, as a consequence of the lacking power surplus evident in Figure 5.3.

GomSpace and ClydeSpace, two well-known cubesat providers, have electrical power system solutions for 3U platforms ranging from 40 to 80 Whr, with possibilities even up to 150 Whr, though at major expense to the volume capacity for other subsystems and payload. An 80 Whr solution uses just under 1U for example [21][22], which is shown to support a 20 W payload if utilising four unfolding solar array wings.

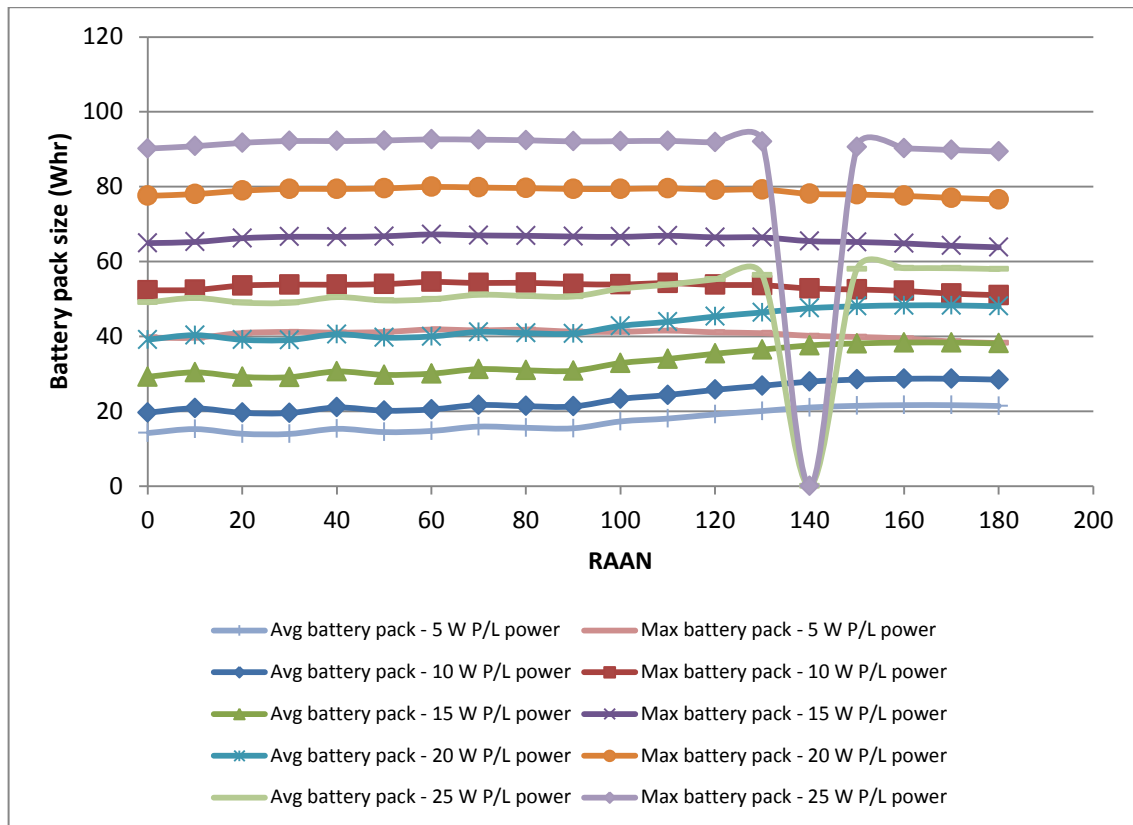


Figure 5.5 Average and maximum battery pack requirement (if derated to 25 % max depth-of-discharge, 100 % redundancy) per year, per RAAN assuming a communication payload power from 5 W – 25 W for the 3U platform with four unfolding wings.

A linear increase in required battery pack with increased payload power consumption is seen, enabling easy extrapolation to other payload power consumptions.

For the power considerations presented so far, the satellite duty cycle is based on the entire duration of satellite access to the area of interest. For the constellation concept presented, multiple satellites have access to the area of interest simultaneously, and satellite handover functionality should ensure that a ground terminal uses the optimal satellite at any given time. As such, the duty cycle of any satellite in the constellation will be shorter than that of a single satellite aiming to serve the area of interest as shown in Figure 5.6 and Figure 5.7.

Figure 5.6 shows the duty cycle of a satellite in the constellation, while Figure 5.7 show the duty cycle of a single satellite, and represents the duty cycle used in the power considerations in this section.

The average and maximum duty cycle of a satellite in the constellation is seen to be ca. 9.6 % and 10.1 % respectively while for a single satellite the equivalent numbers are ca. 16 % and 20 %.

The effect is that the possible payload power consumption presented in this section can be scaled up, and if using the difference in average duty cycle an increase by 66 % is possible.

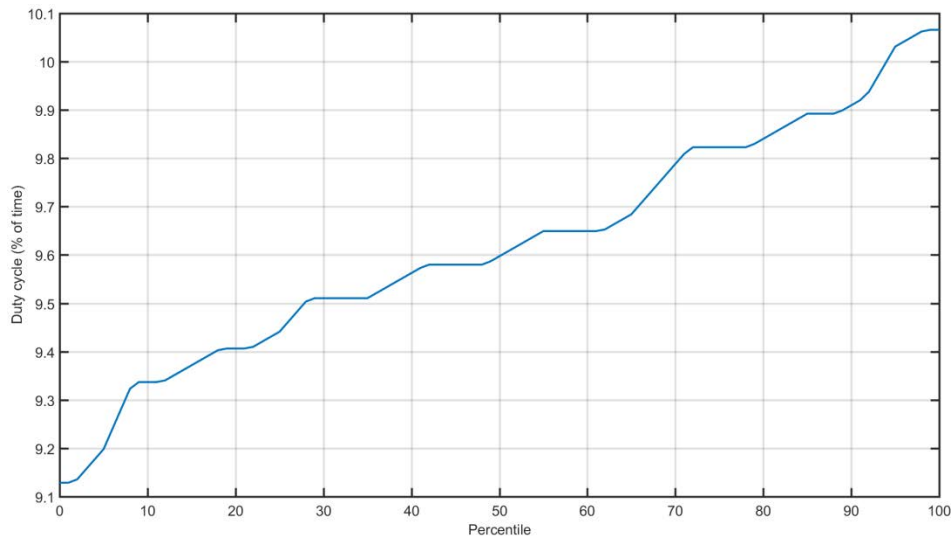


Figure 5.6 Single satellite required duty cycle to cover the area of interest, when operated in a full constellation with handover to the best single satellite, assuming the orbital parameters and elevation constraints in Section 2.

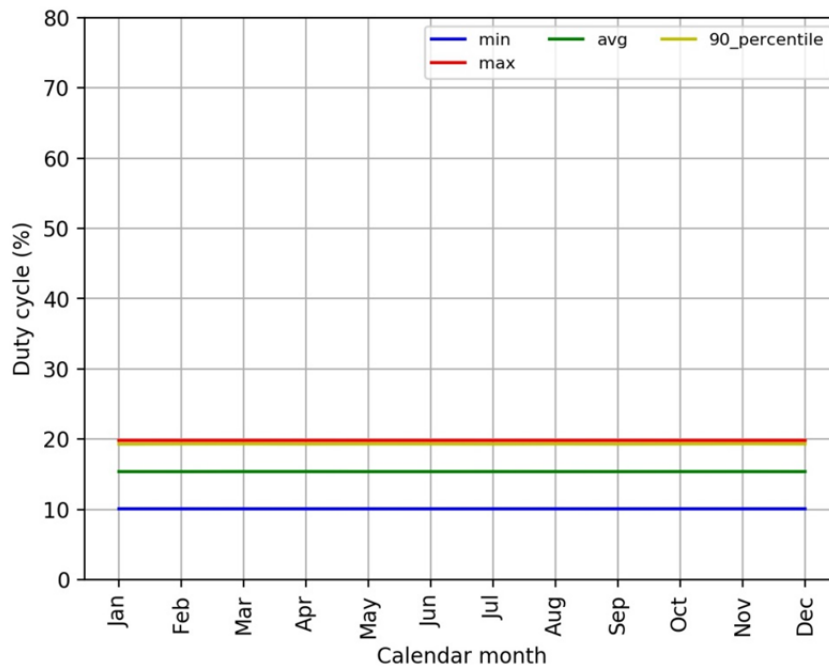


Figure 5.7 Single satellite required duty cycle to cover the area of interest when operated alone, assuming the orbital parameters and elevation constraints in Section 2.

If scaling the results utilising a 10 % duty cycle, both the 5 W and 10 W RF power options can be supported by a 3U platform with four unfolding wings. The average power surplus with two unfolding panels can support the low power option, but there are orbits every year that do not produce enough surplus power.

6 Constellation launch, deployment and maintenance

This chapter evaluates the launch, deployment and orbit maintenance necessary to meet the mission objectives for the proposed satellite constellation. First the major perturbing forces affecting the satellites are discussed and an attempt to estimate the accelerations due to these perturbations is made. The launch opportunities to the mission orbits are then considered and different deployment strategies to distribute the satellites into their correct positions. A simplified velocity change (Δv) budget is drawn up which is used to estimate the size of the on-board propulsion system that is required. Finally some potentially suitable propulsion systems are discussed.

6.1 Perturbations

In a Keplerian orbit, the orbit of a satellite is only affected by the gravitational force of a uniform spherical Earth. Consideration is not given to non-gravitational effects or the gravitational effects of other celestial objects such as the Sun. These effects cause deviations from the Keplerian orbit known as perturbations. Perturbations cause either periodic or secular variations in some or all of the orbital elements. When planning a space mission careful consideration must be given to perturbations, otherwise the position of the satellite will quickly drift from the Keplerian orbit, also known as a reference orbit. The main perturbing effects will now be discussed.

Atmospheric drag

The deceleration due to air molecules is the main non-gravitational force acting on a spacecraft in LEO. The main effect of drag is orbital decay and eventual re-entry. The drag effect is very difficult to predict, primarily due to two factors: drag will vary depending on the shape and attitude of the spacecraft, and the atmospheric density will vary depending on the level of solar activity. Atmospheric drag is the most dominant perturbation for a satellite in LEO, and must normally be actively counteracted to maintain the constellation.

As shown in Appendix A, the counteracting atmospheric drag equates to a maximum yearly correction for altitude maintenance of 11 m/s and a minimum of 0.7 m/s depending on the orientation of the satellite. The maximum reduction in semi major axis due to drag is roughly 20 km per year. A fall in altitude of 50 km will result in a slight degradation of service, but still be acceptable. In order to minimise Δv spend, it may be possible to allow the constellation to degrade due to atmospheric drag and perform altitude maintenance only when the orbit reduces in size beyond a certain limit, perhaps linked to quality of service. This limit would be determined at a later stage of mission planning. In the resulting scenario altitude maintenance would likely be performed no more than once a year for a worst case scenario, or at best no altitude maintenance over the lifetime of the satellite.

Third-body gravitational effects

The gravitational attraction of the Sun and the Moon cause periodic variations in all the orbital elements. These variations are very small for a satellite in LEO, and can be considered negligible at this stage.

Solar radiation pressure

This is pressure exerted on the satellite due to photons radiating from the Sun. It is dependent on the level of solar activity, orientation of the satellite relative to the Sun and the surface reflectivity of the satellite. In LEO and for the proposed satellite to be used in the constellation, its effect is negligible at this phase of the mission planning.

Non-spherical mass distribution / Earth gravity harmonics

A Keplerian orbit assumes a perfectly spherical Earth with a uniform mass distribution. Due to the Earth's rotation on its axis, the Earth's shape is closer to that of an oblate spheroid with a bulge at the equator, and is flatter at the poles. This causes an acceleration to the satellite which can be determined by expanding the geopotential function in a series of spherical harmonics. Detailed discussion and mathematical derivation can be found in [23] [24]. The third expansion term, J_2 , also known as Earth's oblateness, is the dominant term and causes both the right ascension of the ascending node (RAAN) and the argument of perigee to rotate [25].

6.2 Orbital stationkeeping

Orbital stationkeeping are the adjustment manoeuvres necessary to offset the accelerations caused by the perturbations and keep a satellite in a specific desired orbit. This is necessary to maintain the structure of the constellation in order to meet the mission objectives and to avoid collisions with other satellites. There are different parameters that can be used to control the position of the satellites, but for a constellation of satellites in LEO the argument of latitude and the orbital period are two effective and commonly used parameters. The argument of latitude is the argument of periapsis angle plus the true anomaly angle. This can be described as the number of degrees subtended by the satellite since passing the equatorial plane heading North [26]. With perfect stationkeeping, the satellites should be separated by equal angles of argument of latitude, and each orbit should have the same period.

For a constellation of satellites there are two main types of orbital stationkeeping; absolute stationkeeping and relative stationkeeping. Absolute stationkeeping is essentially keeping the satellite within a pre-defined reference frame. The limits of this reference frame are dependent on the mission requirements. Relative stationkeeping, sometimes denoted as formationkeeping, means that the satellite's position is only maintained relative to the other nearby satellites in the constellation. There are advantages and disadvantages to both, depending on the purpose of the mission. An important advantage of absolute stationkeeping is that the constellation pattern is purely deterministic. This means that the projected position of each satellite in the future is

known. This makes the control aspect much simpler compared to relative stationkeeping, where each satellite must know the position of the nearby satellites in the constellation at all times. For the proposed constellation, absolute stationkeeping is considered the most suitable option. Detailed discussion of the advantages and disadvantages of relative and absolute stationkeeping can be found in the literature, see [27].

As noted in Appendix A, as the whole constellation will drift at the same rate, the relative drift is zero and the constellation will retain its shape. It is therefore not necessary to counteract the nodal drift with propulsive effort.

6.3 Velocity change budget

A simplified Δv budget for the scenario in question is shown in Table 6.1 based on the calculations in Appendix A.

Basic Data	
Mission orbit	$a = 6971$ km, $i = 87^\circ$, $e \approx 0$, RAAN = $0^\circ/60^\circ/120^\circ$ (three planes)
Mission duration	5 years
Orbit maintenance requirements	Altitude maintenance, perturbations due to Earth oblateness
Orbit manoeuvre requirements	Phasing manoeuvre (30° in-plane separation)
Final conditions	Earth re-entry
Δv Budget (m/s)	
Orbit Manoeuvres	
In-plane phasing	11
Orbit Maintenance	
Earth Oblateness	N/A
Altitude Maintenance	Mission lifetime: minimum 4 m/s, maximum 55 m/s
Total Δv	66 m/s
Other Considerations	
ADCS	Reaction wheels for attitude control, magnetorquer for reaction wheel desaturation
Margin	Included in propellant budget

Table 6.1 Simplified Δv budget for a single satellite in a LEO constellation.

The on-board propulsion system should be capable of providing a Δv of 66 m/s over the lifetime of the satellite. For a ten year operational lifetime, the total Δv required is approximately 120 m/s. It is estimated that the satellite will require 11 m/s per year to maintain a 600 km altitude. This is a maximum value based on satellite surface area relative to the drag vector and it is reasonable to expect the actual value to be significantly less than this. Additionally, coverage analysis suggests only a slight degradation in service if the satellite altitude is reduced from 600

km to 550 km. The maximum reduction in semi-major axis due to atmospheric drag is 20 km per year. Therefore, it may be possible to devise a schedule for altitude correction where the satellite is allowed to degrade and then boosted back into the desired orbit infrequently, for example once a year. Regardless, there are CubeSat propulsion systems available that are capable of supplying a change in velocity of 120 m/s to a 3U CubeSat. Some of these systems will be considered later in this chapter.

6.4 Launch Opportunities

Today there are two choices when it comes to launching spacecraft; buying an entire launch vehicle, or purchasing some volume on a launch vehicle, also known as ridesharing. The main advantage of a rideshare launch is that it is inexpensive compared to purchasing a dedicated launch. The main disadvantages are that you normally cannot select the specific destination orbit, or decide the time and date of the launch. For this study, cost effectiveness is a priority so ridesharing opportunities are considered in more detail. Additionally, small satellite launchers are briefly discussed due to their potential for providing a low cost dedicated launch vehicle alternative in the near future, potentially enabling constellation optimisation after one or two shared launches. Spaceflight is an example launch services provider that offers rideshare opportunities. They publish their schedule and this shows a number of opportunities over the next three years to rideshare on a launch to LEO, especially to SSO [28]. Launching 30 3U CubeSats at a total weight of 120 kg with a single rideshare launch is viable, in terms of mass and volume. The challenge will be releasing the satellites into three different planes, and this will likely be a prohibiting factor for the single launch strategy to be viable, as discussed section 6.4.2.1.

6.4.1 Dedicated Launch

This section will briefly consider dedicated small satellite launch vehicles. There are currently no suitable launch vehicles in this category, but there is significant activity in this area, and the progress being made suggests this may become a viable option for launching small satellites in the near future. The main challenges for the developers of these launch vehicles are cost reduction and technology demonstrations in order to show that these launch vehicles can become a real alternative to traditional launch vehicles. Some noteworthy actors in the market are Virgin Orbit, Vector Space Systems and Rocket Lab. Rocket Lab appears to have reached the furthest in their development, having already conducted one test flight with plans for at least one further test [29]. In Norway, there is a European Union Horizon 2020 project called ‘SMILE’ (SMall Innovative Launcher for Europe), which plans to develop a launcher for satellites up to 50 kg which will launch from Andøya Space Centre [30]. A small satellite launcher has the same advantages as a traditional launcher, but is designed for a smaller payload. A more detailed discussion on small satellite launchers can be found in Appendix D.5 in [1]. The small satellite market is increasing, and there is a need for more launch opportunities. There are also many payloads that have strict requirements in terms of orbit and timing of launch. Dedicated small satellite launch vehicles may well provide a solution to these challenges and the development of this market should be monitored closely.

6.4.2 Deployment Strategies

This section will discuss some common strategies for the deployment of a constellation of satellites in LEO utilising ridesharing opportunities. Important factors to consider when choosing the deployment strategy are:

- Launch cost and opportunity
- Separation scheme
- Time
- Propulsive requirements
- Flight heritage of method

6.4.2.1 Cluster launch of entire constellation

All the satellites in the constellation are launched together. There are a few options for deployment in this scenario:

1. On-board propulsion system
2. Nodal precession
3. A manoeuvrable launch vehicle upper stage combined with a multi-payload adapter (MPA)

Detailed discussion of this scenario and the three deployment strategies listed can be found in Appendix A. In summary, launching the entire constellation on a single launch vehicle faces challenges which make this strategy unviable. For option 1, an on-board propulsion system is not capable of the large orbital manoeuvres required for deployment to the different mission orbits. For option 2, nodal precession will require several years before correct separation is achieved. For option 3, it is unlikely launch vehicle upper stages can manoeuvre between the different orbital planes, and it will also require the launch vehicle to carry much more fuel which may be an obstacle, particularly as a secondary payload.

6.4.2.2 Cluster launch per plane

All the satellites in each plane are launched together, with a propulsion system on-board each satellite to perform in-plane phasing. This is likely the most feasible strategy to launch and deploy the constellation within a reasonable time frame. As a secondary payload, obtaining three separate launches going to the desired orbit is challenging, and it may take years before the constellation is fully deployed. Compromises should be considered if possible, for example on altitude or inclination, in order to deploy the entire constellation as soon as possible. In order to more accurately determine the possibility of launching the constellation in this manner, commercial launches from the past three years were collected. This data was filtered on altitude and inclination to only include launches going to a suitable orbit for the constellation. The results are in Figure 6.1. This shows that although the number is restricted, there are several

opportunities to rideshare to a suitable orbit. Additionally, the number of launches to LEO orbits seems to be increasing, and all the launches listed in the table carried secondary payloads. The launches are also going to a number of different planes, as illustrated in Figure 6.1. There may also be the possibility of ridesharing with launch vehicles that have a military payload, which are not included in the table, thus increasing the number of potential suitable launches. Historical evidence suggests that with careful planning and possibly some compromises on destination orbit, it is possible to launch the entire constellation via ridesharing.

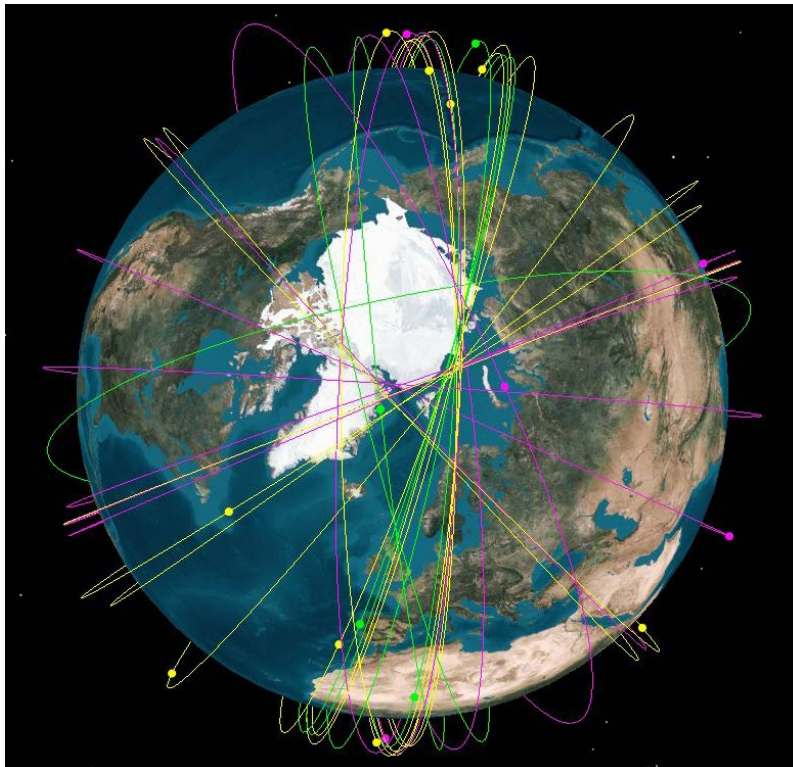


Figure 6.1 The orbits attained by the satellites on-board suitable launches from January 2015 until September 2017. The figures illustrate the various planes the satellites have been released into.

6.4.3 Summary of launch strategies

Launching the entire constellation with a single launch vehicle is not feasible as the on-board propulsion system cannot perform a large out-of-plane manoeuvre. Launching the satellites individually means it will likely take several years before for the entire constellation is deployed. A good solution may be to cluster launch all the satellites in the same plane. An on-board propulsion system would then be used to separate the satellites in each plane. There are a number of opportunities to rideshare either to or close to the desired mission orbits. A combination of rideshare and dedicated launches may facilitate better optimisation of the resulting constellation, and allow full deployment to be achieved sooner. If dedicated small

launchers do not become a viable alternative, compromises on the destination orbit should be considered in order to achieve full deployment within a reasonable timeframe.

6.5 On-board propulsion system

The propellant mass required to meet the Δv requirements have been estimated in Appendix A. For a propulsion system with a specific impulse of 200 s, approximately 130 g of propellant would be required to deliver a change in velocity of 66 m/s to a CubeSat with an initial mass of 4 kg.

6.5.1 Potential propulsion systems

The propulsion system on-board each satellite must be capable of a total lifetime Δv requirement of approximately 66 m/s for a five year mission, and 120 m/s for a ten year mission. It must also meet the power, volume and mass restrictions of the satellite platform. There are a number of systems, both chemical and electric propulsion systems that appear able to meet these requirements. Electric propulsion systems typically have high efficiency and high performance. However, electric systems generally become less efficient when miniaturised, and have high power requirements compared to chemical systems of comparable size. Chemical systems have higher thrust and greater flight heritage, but lower efficiencies than electric systems. A more detailed discussion of different propulsion systems can be found in [1]. Two propulsion systems that may be suitable are:

1. VACCO AFRL Propulsion Unit for CubeSats (PUC) [36]
2. Busek Electrospray Thruster (BET) 1mN [37]

The AFRL PUC system uses 15 W in firing mode and 0.055 W in standby. It is scalable, and the 1U version is capable of providing a Δv of 167 m/s to a CubeSat with mass of 4 kg. This system uses sulphur dioxide as propellant in warm gas mode, but is also available in a cold gas version using R-236fa as propellant. An alternative, electric propulsion system is the BET-1mN system from Busek. It is based on the BET-100 which performed successfully on the ESA LISA Pathfinder mission. This system uses 15 W in firing mode and an ionic liquid as propellant. For a 4 kg CubeSat it is capable of a change in velocity of 151 m/s. Micro propulsion systems are primarily used for stationkeeping or as part of the ADCS.

The technical challenge with micro propulsion is miniaturising systems whilst maintaining good performance. Another challenge is a lack of demonstration flights. The two systems discussed here are based on larger propulsion systems that have flight heritage, but neither of these systems have, to the authors' knowledge, been demonstrated in space. There is a growing need for propulsion systems for small satellites and there is significant development in this area with systems at various levels of maturity [38]. High performance micro propulsion systems will likely become available in the near future, capable of major orbital manoeuvres such as inclination changes.

6.6 Summary launch and orbit maintenance

The main perturbation which needs to be counteracted is atmospheric drag. The orbit decay rate is dependent on a number of factors including solar activity and spacecraft attitude. Assuming mean solar activity and constant maximum surface area perpendicular to the drag vector, a yearly altitude correction of 11 m/s is required. Left uncorrected, this orientation will result in a shrinking of the orbit due to drag by approximately 20 km per year. A reduction in altitude of 50 km from 600 km to 550 km will result in a slight degradation of service, but still acceptable. In order to minimise Δv spend, it may be possible to allow the constellation to degrade due to atmospheric drag and perform altitude maintenance only when the orbit shrinks beyond a defined limit. Earth's non-spherical mass distribution will also cause deviations from the reference orbit, causing nodal drift. Since all the satellites will experience this drift, the relative drift is zero and it won't be necessary to counteract this perturbation.

A Δv budget has been calculated. There are three main operations included in the budget: a phasing manoeuvre, altitude maintenance over the lifetime of the satellite and end-of-life disposal. For a five year mission, the maximum required Δv is approximately 92 m/s, for ten years it is 120 m/s. An on-board propulsion system will be used to perform the operations necessary manoeuvres and orbital maintenance.

The most viable strategy for launching the constellation is to launch all the satellites in the same plane together, then use on-board propulsion to achieve the correct in-plane separation between the satellites. This strategy will require three separate launches, and deployment of the entire constellation will likely take some time depending on the availability of suitable rideshare launches. Dedicated small satellite launch vehicles may provide an alternative to ridesharing in the near future, which will permit a much shorter deployment time.

7 Summary

A coverage analysis was carried out to identify a suitable LEO constellation. Near continuous coverage was required within an area defined by a polygon covering the main Norwegian interest areas. With a nominal orbital altitude of 600 km, a Walker Star constellation with a total of 30 satellites in 3 orbital planes and an inclination of 87 degrees provided sufficient coverage when requiring a minimum elevation angle of 5 degrees. The effect of varying the orbital altitude between 500 and 650 km was found to marginally change the degree of coverage, enabling a wider range of launch options. Sun synchronous orbits having an inclination of about 98 degrees reduced the coverage, especially in the southern part of the coverage area. The most critical parameter identified was plane separation, where ideally the planes are equally spaced with 60 degrees separation.

Launch and orbit maintenance was investigated for a 3U platform size. The required velocity change for plane separation implies the necessity of separate launches per plane. Dedicated launches might become economically feasible in the future, however, currently ridesharing seems to be the most viable option. Investigation of past LEO launches to near polar orbits indicates that over a period of a few years it should be possible to obtain close to desired plane separation with ridesharing, thereby obtaining reasonably good coverage. It may also be possible to utilise two shared launches, and one dedicated launch, in order to ensure an optimum final constellation within a shorter timeframe. Calculations of the total velocity change required over the lifetime of the satellite is within the capability of current propulsions systems available for nanosatellites, assuming a system operational time duration of 5 to 10 years.

We have assumed two payload variants for nanosatellites: a low power option with 5 W linear signal power from the satellite HPA and a high power option with 10 W available. With an efficiency of 33 %, this translates to a DC power consumption of 15 or 30 W. Allowing some power to other payload components results in a total power consumption in order of 18-20 W for the low power version and 33-35 W for the high power variant. The duty cycle of the payloads is on average 9.5 % and 10 % duty cycle has been assumed. Additional power consumption from the attitude determination and control system, computing system etc. is accounted for by including 4 W when the satellite is not active and additional 3 W when the satellite is active. Simulations of a 3 U platform with 4 unfolding wings and a 80 Whr battery pack is able to support a 33 W payload power given a 10 % duty cycle. This initial investigation shows that the high power payload option is within reach of a 3U satellite.

The communication system capacity within the coverage area, given a number of assumptions, range from 109 Mbit/s at X-band, 93 Mbit/s at Ku-band and 52 Mbit/s at Ka-band for the high power payload option. For the low power option about half of the capacity is achievable.

8 Comparison with highly elliptical orbit

In the previously reported HEO study [1] the feasibility of utilising 3 microsattellites for provisioning of broadband high latitude services was investigated. The payload power consumption was assumed to be in the range 100 W, with a significantly higher duty cycle compared to the current LEO constellation of 30 nanosatellites.

Cost estimates for both the ground and space segment is necessary before drawing a final conclusion on the preferred orbital type. Some technical considerations to take into account are detailed below.

8.1 Launch and propulsion

For the HEO constellation direct launch to the desired orbits as a secondary payload was found to be the most viable launch option. Launching as a secondary payload and carrying an on-board propulsion system capable of manoeuvring into the desired orbit seems the most flexible option in terms of launch cost and availability. However, there are currently no commercially available propulsion systems suitable for microsatellites capable of performing the orbit transfer, but the current technology trends suggest that a suitable electric propulsion system is likely to be available in the near future years.

For the currently investigated LEO constellation the most viable strategy for launching the constellation is to launch all the satellites in the same plane together, then use on-board propulsion to achieve the correct in-plane separation between satellites. This strategy will require three separate launches, and deployment of the entire constellation will likely take some time. Dedicated small satellite launch vehicles may provide an alternative to ridesharing in the near future, which will permit a much shorter deployment time and ideal mission orbits. The number of possible rideshare launches is significantly less for HEO orbits compared to near polar LEO launches, and our impression is that the challenge of obtaining launch opportunities is less for a LEO constellation.

8.2 Spacecraft

The effort required to produce 3 microsatellites intended for HEO operation tolerating the increased space radiation environment is foreseen to be a challenge, especially if low cost commercially available components are to be utilised. The volume production of 30 smaller nanosatellites intended for LEO operation is perceived as a significantly less challenging, as most of the components are already flight proven.

The LEO constellation will degrade more gracefully if errors occur on one or more spacecraft due to the larger number of satellites in the constellation compared to the HEO constellation. Both constellations provide coverage also outside the investigated area, however, worldwide coverage will be better for the LEO constellation than for the HEO constellation.

8.3 System capacity and ground segment

If comparing the results found for transparent transponders in the HEO study [1], the 5 W satellite transmit power case with 30 satellites has similar capacity as obtained by 3 HEO satellites each with 23 W available signal power (49 Mbit/s at X-band, 47 Mbit/s at Ku-band and 29 Mbit/s for Ka-band). One significant difference is the faster decrease of capacity with increasing frequency for the LEO case compared to the HEO case when comparing the 3 frequency bands. This is caused by frequent occurrence of low elevation angles for the LEO case, resulting in increased excess attenuation and free space loss. Another difference is the limitations at Ka-band observed in the LEO case, where a combination of the selected satellite

antenna solution and user terminal characteristics imposed a limit on the available bit rate available for each terminal; this was not observed for the HEO case.

At X- and Ku-bands, 3 satellites with transparent transponders utilising a payload power of about 100 W provides about the same system capacity as 30 smaller LEO satellites utilising the low power payload option of 16 - 20 W.

The ground segment for the LEO constellation requires two gateways to provide continuous coverage, while one gateway is sufficient for the HEO constellation. The southern LEO gateway is required to have two tracking antennas, while the northern needs 4 tracking antennas. In comparison, two tracking antennas should be sufficient for the HEO solution.

For both constellation types tracking user terminal antennas are required. The network control is required to handle frequent handovers in the LEO case; handovers occur less frequently for HEO. To avoid interrupts during handovers the users are required to employ two tracking antennas simultaneously. Doppler frequency shifts need to be handled in both cases. The time percentage with high elevation angle towards the serving satellite is presumably significantly larger for HEO compared to LEO, implying improved service availability for mobile users with fewer obstacles hindering the communication in the HEO case.

9 Conclusions

This study considered the feasibility of utilising a constellation of small satellites in low Earth orbits for continuous broadband communications in Norway and the Arctic. Three different frequency bands, X, Ku and K/Ka within the frequency range 7.25 - 31 GHz have been used as examples for both commercial and governmental services. The user equipment example represents a vehicular terminal with antenna diameter of 80 cm. A low cost gateway antenna size of 3 m is assumed. Coverage calculations showed that the area of interest could be continuously covered by 30 satellites divided in 3 planes at an altitude of 600 km.

With about 20 W available for the payload during the active period, corresponding to approximately 5 W transmit power, transparent transponders can offer a system capacity of about 51 Mbit/s at X-band, 42 Mbit/s at Ku-band and 25 Mbit/s at Ka-band. With about 35 W payload power and a corresponding RF power of 10 W, allowed by the calculated power budget, the system communications capacity is estimated to 109, 93 and 52 Mbit/s at X, Ku- and Ka-band, respectively. Capacity increase may be obtained by utilising more advanced technology, such as on board processing and satellite antenna spot beams, as well as by increasing the solar panel size, and thus available payload power.

Additional power consumption from the attitude determination and control system, computing system etc. is accounted for by including 4 W when the satellite is not active and additional 3 W when the satellite is active. Simulations of a 3U platform with 4 unfolding wings and an 80 Whr battery pack is able to support close to 35 W payload power given a 10 % duty cycle.

Launch possibilities, orbit maintenance requirements and propulsion systems were investigated for a 3U platform. The required velocity changes for deploying into three separate planes implies the need for one launch per plane. Dedicated launches with small launch vehicles may become an economically feasible alternative in the near future, however, currently ridesharing is the most viable option. Investigation of past LEO launches to near polar orbits indicates that over a period of a few years it should be possible to obtain close to desired plane separation with ridesharing. An on-board propulsion system is used to separate the satellites in each plane, for orbit maintenance and for deorbiting, if necessary. The orbital manoeuvres and corrections required for a five to ten year mission is within reach of current propulsion systems available for nanosatellites. A five year mission would require approximately 92 m/s, and a ten year mission approximately 120 m/s. The lifetime velocity change requirement can be reduced, depending on the level of orbital maintenance that is deemed required.

The study concludes that current nanosatellite technology is able to support relevant communication capacity for continuous Arctic coverage utilising a constellation of LEO satellites. Availability of launches to the desired orbits is expected to be possible, and the space radiation risk is significantly lower compared to highly elliptical orbiting satellites. We recommended carrying out a feasibility study, in cooperation with vendors, to determine if utilisation of small satellites is a cost effective solution for a regional broadband system.

Appendices

A Orbital manoeuvres, propulsion systems and launch opportunities - equations and background

A.1 Assumptions

Orbit and constellation parameters

Altitude (circular orbit) = 600 km

Inclination = 87°

Separation in RAAN between the orbital planes: 60°

Separation in true anomaly between satellites in each plane: 30°

Satellite (3U CubeSat with deployable solar panels)

Mass = 4 kg

Volume = 3 litres

Surface area (minimum) = 0.01 m^2

- Minimum – Assuming solar panels deployed and moving parallel relative to drag vector. The surface area for the solar panels is assumed negligible in this orientation.

Surface area (maximum) = 0.16 m^2

- Maximum – Assuming solar panels deployed and moving at right-angle relative to drag vector.

A.2 Atmospheric drag

The following formula estimates the change in velocity required per orbit to counteract the loss in altitude due to atmospheric drag:

$$\Delta V_{rev} = \pi \left(\frac{C_D A}{m} \right) \rho a V \approx 2 * 10^{-4} m/s \quad (A.1)$$

where

Mean atmospheric density, $\rho = 1.37 * 10^{-13} \text{ kg/m}^3$ (assuming mean solar activity)

Assuming maximum surface area, $A_{max} = 0.16 \text{ m}^2$

Coefficient of drag, $C_D \approx 2.2$

Semi-major axis, $a = 6971 \text{ km}$ (600 km altitude)

Orbital velocity, $V = 7.56 \text{ km/s}$

This equates to a maximum yearly correction for altitude maintenance of **11 m/s** and a minimum of **0.7 m/s** depending on the orientation of the satellite.

A.2.1 Reduction in semi-major axis due to atmospheric drag

The following formula estimates how much the semi-major axis will reduce per revolution due to atmospheric drag.

$$\Delta a_{rev} = -2\pi \left(\frac{C_D A}{m} \right) \rho a^2 \quad (A.2)$$

$$\Delta a_{(max)} \approx -20 \frac{km}{year}$$

$$\Delta a_{(min)} \approx -1.25 \frac{km}{year}$$

A fall in altitude of 50 km will result in a slight degradation of service, but still acceptable. In order to minimise Δv spent, it may be possible to allow the constellation to degrade due to atmospheric drag and perform altitude maintenance only when the orbit shrinks beyond a specified limit. This limit would be determined at a later stage of mission planning. It should be noted that the analytical method employed here is only an estimate. For example, it is assumed that the density is constant, but as the altitude of the satellite decreases the density increases and the satellite falls at a faster rate. The values for density are obtained from the NRLMSIS-00 atmosphere model which is based on empirical data. The difference in density at 600 km and 580 km is of a small magnitude, and will not significantly impact the reduction in semi-major axis estimated above. As such it is acceptable for this phase of mission planning. A numerical method, solving the equations of motions to get an approximation of the satellite's motion, may provide a better estimate and should be performed in the next phase of planning, along with a detailed mission profile.

A.3 Earth's oblateness

It is possible to express nodal drift rate as a function of semi-major axis, inclination and eccentricity:

$$\dot{\Omega}_{J_2} = -1.5nJ_2 \left(\frac{R_E}{a}\right)^2 \cos i (1 - e^2)^{-2} \quad (\text{A.3})$$

where n is the mean motion in deg/day

$$n = \frac{360^\circ}{P} \quad (\text{A.4})$$

and P is the time period to complete one orbit. The mean motion at 600 km altitude is:

$$n = 5370 \frac{\text{deg}}{\text{day}} \quad (\text{A.5})$$

and the nodal drift rate is:

$$\dot{\Omega}_{J_2} = -\frac{3}{2}J_2 \left(\frac{R_E}{a_1(1-e_1^2)}\right)^2 n \cos i \approx -0.4 \frac{\text{deg}}{\text{day}} \quad (\text{A.6})$$

As the whole constellation will drift at the same rate, the relative drift is zero and the constellation will retain its shape. It is therefore not necessary to counteract the nodal drift with propulsive effort.

A.4 Phasing manoeuvre

It is possible to estimate the Δv required to perform the phasing manoeuvre in order to achieve correct separation between the satellites in each plane, and to estimate how long it will take to perform the manoeuvre. This manoeuvre typically involves changing the orbit of one of the satellites, referred to as the interceptor, so it drifts at a different rate to the target satellite. It remains in this interceptor orbit until the desired separation to the target satellite is achieved. The satellite is then manoeuvred back to the target orbit. In the equations below, the subscript 'tgt' refers to the orbit of the target satellite, and the subscript 'int' refers to the orbit of the interceptor satellite. k_{int} is the number of orbits the interceptor satellite makes in the interceptor orbit, and k_{tgt} the equivalent for the target satellite.

Mean motion at 600 km altitude

$$\omega_{tgt} = n_{tgt} = 0.06 \frac{\text{deg}}{\text{s}} = 1.1 * 10^{-3} \frac{\text{rad}}{\text{s}} \quad (\text{A.7})$$

$$k_{\text{int}} = k_{\text{tgt}} = 50$$

$$\tau_{phase} = \frac{2\pi k_{tgt} + \vartheta}{\omega_{tgt}} = 290207 \text{ s} \quad (\text{A.8})$$

$$a_{phase} = \left(\frac{\tau_{phase} \sqrt{\mu}}{2\pi k_{int}} \right)^{2/3} = 6980 \text{ km} \quad (\text{A.9})$$

$$\Delta V_1 = \left| \sqrt{\frac{2\mu}{a_{tgt}} - \frac{\mu}{a_{phase}}} - \sqrt{\frac{\mu}{a_{tgt}}} \right| = 5.1 \text{ m/s} \quad (\text{A.10})$$

$$\Delta V = 2 * |\Delta V_1| \approx 11 \text{ m/s} \quad (\text{A.11})$$

The manoeuvre will take approximately 81 hours. With ten satellites in each plane, it will take just over 30 days for all the satellites in each plane to attain their correct position.

A.5 Deorbit

The end-of-life strategy will be an uncontrolled deorbit, and the satellite will burn up in atmosphere upon re-entry. It is assumed that the constellation will decay naturally within 25 years after mission completion. This means a deorbit strategy that necessitates propulsive capability is not required. Thus deorbiting is not included in the delta-v budget. However, orbit lifetimes are dependent on many factors, including solar activity and orientation of the satellite relative to the drag vector. This makes lifetime difficult to predict and 600 km is on the limit of the rule-of-thumb for natural decay within 25 years. This section therefore estimates how much delta-v would be required to lower the altitude of constellation to 550 km, an altitude from which the satellite will almost certainly decay within 25 years.

Change in velocity required to manoeuvre the satellite from an altitude of 600 km to 550 km

$$|\Delta V_1| = \left| \sqrt{\frac{2\mu}{r_1} - \frac{\mu}{a}} - \sqrt{\frac{\mu}{r_1}} \right| = 13.6 \text{ m/s} \quad (\text{A.12})$$

$$|\Delta V_2| = \left| \sqrt{\frac{\mu}{r_2}} - \sqrt{\frac{2\mu}{r_2} - \frac{\mu}{a}} \right| = 13.6 \text{ m/s} \quad (\text{A.13})$$

$$\Delta V_{Total} = \Delta V_1 + \Delta V_2 \approx 27 \text{ m/s} \quad (\text{A.14})$$

It is estimated that it will require 27 m/s to manoeuvre from the mission orbit to an orbit from which the satellite will re-enter the atmosphere within 25 years. A computer model of the orbital decay will give a better estimate of the orbital lifetime of the satellite and should be performed in later stages of development.

A.6 Cluster launch of entire constellation

A.6.1 On-board propulsion system

The propulsion system on-board the satellite would have to be capable of a large plane change manoeuvre and a phasing manoeuvre as well as stationkeeping. The satellites are configured into three separate planes, with the longitude of the ascending node between the planes separated by 60° . For circular orbits of the same size, the Δv required to perform the plane change can be determined by

$$\Delta V = 2V \sin\left(\frac{\alpha}{2}\right) \quad (\text{A.15})$$

Where V is the orbital velocity and α is the plane change angle. A plane change of 60° will require a change in velocity equal in magnitude to the orbital velocity of the satellite. For a satellite in a 600 km circular orbit, this is approximately 7.55 km/s. This is beyond the capability of current CubeSat propulsion.

A.6.2 Nodal precession

Different orbits precess at different rates due to Earth's oblateness. Using Equation A.6, it is possible to calculate the differential drift between two orbits. This can then be used to perform in-plane manoeuvres to separate the orbits of the satellites in RAAN and true anomaly. As an example, assume a drift orbit of 800 km.

Mean motion at 800 km

$$n = 5147 \frac{\text{deg}}{\text{day}} \quad (\text{A.16})$$

Drift rate at 800 km

$$\dot{\Omega}_{J_2} = 0.36 \frac{\text{deg}}{\text{day}} \quad (\text{A.17})$$

Then calculate the differential drift rate between the 600 km orbit and 800 km orbit

$$(\Delta \dot{\Omega}_{J_2})_{1 \rightarrow 2} = (\dot{\Omega}_{J_2})_1 - (\dot{\Omega}_{J_2})_2 = 0.016 \quad (\text{A.18})$$

The drift time to achieve a 60° separation in RAAN is then

$$t_{\text{drift}} = \frac{\theta_{\text{sep}}}{\Delta \dot{\Omega}_{J_2}} \approx 10 \text{ years and 5 months} \quad (\text{A.19})$$

Where

θ_{sep} = angular separation between the two planes

Since it will take over ten years to achieve the desired separation, it is clear that relying solely on nodal precession is not an effective strategy for deployment. Furthermore, additional propulsive capability is required to transfer the satellite from the drift orbit to the mission orbit when the desired separation is achieved.

A.6.3 Manoeuvrable launch vehicle upper stage combined with a MPA

There are several launch vehicles with upper stages capable of manoeuvring to the desired orbital planes. An example is a Soyuz-2 rocket with a Fregat upper stage. There are also several MPAs capable of deploying CubeSats. An example is an ESPA ring with ten P-PODs mounted [39]. This configuration would be capable of deploying ten 3U CubeSats. Furthermore, the ideal MPA or MPA mount should have some form of propulsive capability that allows for in-plane separation in order to further reduce the complexity of the on-board propulsion system. Puig-Suari simulated that it's possible to deploy a CubeSat constellation in 45 days without CubeSat propulsion [40]. In-plane separation is achieved by releasing the satellites with different separation speeds using a differential spring energy dispenser, instead of simply relying on different separation times to avoid collision. This separation will remain for a few weeks, but in order to maintain the constellation over several years, a propulsion system is necessary. In this case, the Δv requirement to “freeze” the orbit is small (maximum 7.4 m/s) and can be achieved using current CubeSat propulsion technology. Launching and deploying in the manner described is technically feasible, but the practical implementation will be challenging. The main problem is manoeuvring between the different orbital planes. Launch mission profiles do not usually involve large changes in inclination or longitude of the ascending node. This is because of the high Δv required to perform such manoeuvres, which requires the launch vehicle upper stage to carry additional fuel in order to perform. Launch vehicle upper stages may significantly raise or lower the orbit to release different payloads at different altitudes, but normally only very small plane changes are executed. This will likely be a prohibiting factor to launching the constellation all at once, especially as a secondary payload.

A.7 Propulsion system requirements

Attitude control will be performed by an ADCS separate from the primary propulsion system. The main tasks for the propulsion system will be to perform the spacing manoeuvre and orbital maintenance. Altitude maintenance and deorbiting are included in the Δv budget, but this may not be required, or required to a lesser degree than estimated in the Δv budget. It is not necessary to counteract drift in the RAAN, as the rate of drift will be the same for all the satellites. The size of the required propulsion system can be estimated by:

$$\Delta v = v_e \ln \frac{m_0}{m_f} \quad (\text{A.20})$$

Where

$$v_e = I_{sp} * g_0 \quad (\text{A.21})$$

$$m_f \equiv m_0 - m_p \quad (\text{A.22})$$

$$\Delta v = g_0 * I_{sp} * \ln\left(\frac{m_0}{m_0 - m_p}\right) \quad (\text{A.23})$$

An alternative form of the equation makes it possible to determine the propellant mass fraction required

$$m_p = m_0 \left[1 - e^{-\left(\frac{\Delta V}{I_{sp} g_0}\right)} \right] \approx 0.13 \text{ kg} \quad (\text{A.24})$$

Where

g_0 (m/s²) is the acceleration at the Earth's surface

I_{sp} (s) is the specific impulse

m_0 (kg) is the initial total mass including propellant, also known as wet mass

m_f (kg) is the final total mass without propellant, also known as dry mass

m_p (kg) is the propellant mass

v_e (m/s) is the effective exhaust velocity

ΔV (m/s) is the total change of velocity of the vehicle (with no external forces acting)

Assuming a specific impulse of 200 s, the propulsion system would need 130 g of propellant to meet the lifetime Δv requirement for each satellite in the constellation. This is within the capability of several available CubeSat propulsion systems.

A.8 Launch

In order to determine the possibility of launching as a secondary payload to the desired orbits, a search of commercial launches in the past three years was performed with the following criteria:

- launch must have had a secondary payload on-board
- inclination between 80 and 100 degrees
- altitude between 500 and 700 km

Year	Number of suitable launches
2015	10
2016	15
2017 (as of 1 st September 2017)	7

Table A.1 Summary of suitable commercial launches for the constellation from the past three years.

B Spacecraft mass and power budget

The required technologies of Section 5.1 yield implied power and mass budgets of the order shown in Table B.1, before sizing the payload system, and are estimated by FFI to be within the scope of a small satellite mission. For the propulsion unit power, only standby power is accounted for, since the required firings are so seldom and of short duration, see Section 6, that it has very little impact on an average power budget such as that in Table B.1. However, the power system must be scaled to be able to supply the peak power required by the propulsion unit. At the current stage, the peak power of the payload is believed to be of the same order or greater than that of the propulsion unit so if the power system can handle the payload it can handle the propulsion unit, though not necessarily simultaneously.

The battery weight listed assumes an 80 Whr battery pack.

Unit	No. units	Transponder inactive power (W)	Transponder operations power (W)	Mass (kg)
Attitude Determination and Control System				
Magnetometer	1	0.45	0.45	0.2
Propulsion unit	1	0.055	0.055	0.6
Sun Sensors	6	0.03	0.03	0.03
Rate sensor	1	0.33	0.33	0.1
Actuator	3	0.54	0.54	0.36
Magnetorquer	3	0.6	0.6	0.09
ADCComputer	1	0.5	0.5	0.05
Sum		2.775	2.775	1.43
Communication System				
UHF Rx	1	0.25	0.25	0.245
UHF Tx	1	0	2.64	
Sum		0.25	2.89	0.245
Payload System				
Payload system	1	TBD	TBD	TBD
Payload antenna	1	0	0	TBD
Payload computer	0	0	0.5	0.05
Sum			TBD	TBD
Computing system				
HKC computer	1	0.5	0.5	0.05
Storage unit	1	0.15	0.15	0.061
Sum		0.65	0.65	0.111
Power system				
Power system	1	0.5	0.5	0.05
Sum		0.5	0.5	0.05
Spacecraft total				
Cables				0.15
Structure				0.35
Batteries (80 Whr)				0.53
Solar panels (body)				0.5
Solar panels (wing)	2-4			0.125 – 0.5
		Transponder inactive power (W)	Transponder operations power (W)	Mass (kg)
Sum		4.175	6.815	3.49 – 3.87

Table B.1 Spacecraft sub-system power and mass estimation. Note that the power and mass of the transponder is not included yet, nor is the mass of the payload antenna, batteries or solar panels, which depend on the final transponder and orbit configuration. The propulsion system that may be required to get into orbit, depending on launch configuration, is not included either.

C Radiation

The protons are concentrated in the inner belt, between 500 km and 15 000 km above Earth's surface, see Figure C.1. In the figure a radius of one corresponds to the Earth's radius with the North Pole on the upper left side.

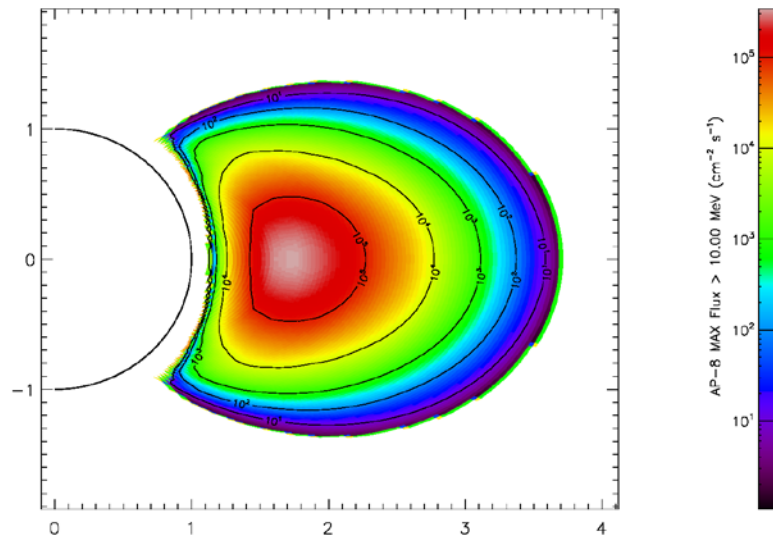


Figure C.1 Map of proton flux for energies above 10.0 MeV in a time of solar maximum. The circle to the left represents the Earth's surface. The vertical axis represents the direction of Earth's magnetic field and the units on the axis are equal to the radius of Earth. Generated and plotted with SPENVIS by the use of the AP-8 MAX model.

The electrons are distributed over a larger area that reaches out to 60 000 km above Earth's surface, but is concentrated in two belts, see Figure C.2. These are the inner belt, where also the protons are concentrated, and the outer belt between 15 000 km and 60 000 km.

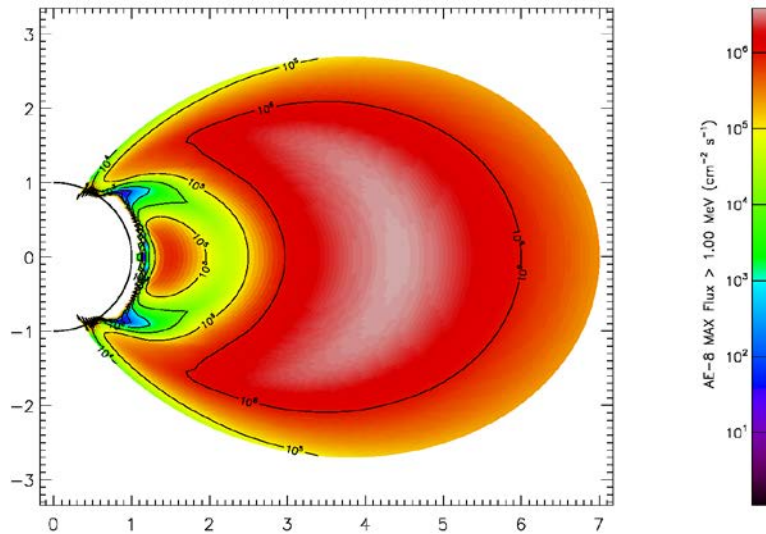


Figure C.2 Map of the electron flux for energies larger than 1.0 MeV in a time of solar maximum. The circle to the left represents the Earth's surface. The vertical axis represents the direction of Earth's magnetic field and the units on the axis are equal to the radius of Earth. Generated and plotted with SPENVIS by the use of the AE-8 MAX model.

When studying the Van Allen belt it is important to take account of the solar cycle because of its influence on the flux in the belt, especially in the inner belt [31]. The solar cycle has a period of about 11 years. The last solar maximum occurred in April 2014, and the next solar maximum is expected to occur in the first half of the 2020s [32] and is expected to be weak [33].

Because of the separation of the Earth's rotational axis and magnetic axis we get zones where the inner Van Allen belt reaches down to low altitudes [7]. As a consequence of this we have a zone in the southern Atlantic Ocean, called the South Atlantic Anomaly (SAA), where the radiation belt reaches down to 200 km above the surface, see Figure C.3. For the electrons we get in addition zones at latitudes of 60° north and 60° south, see Figure C.4.

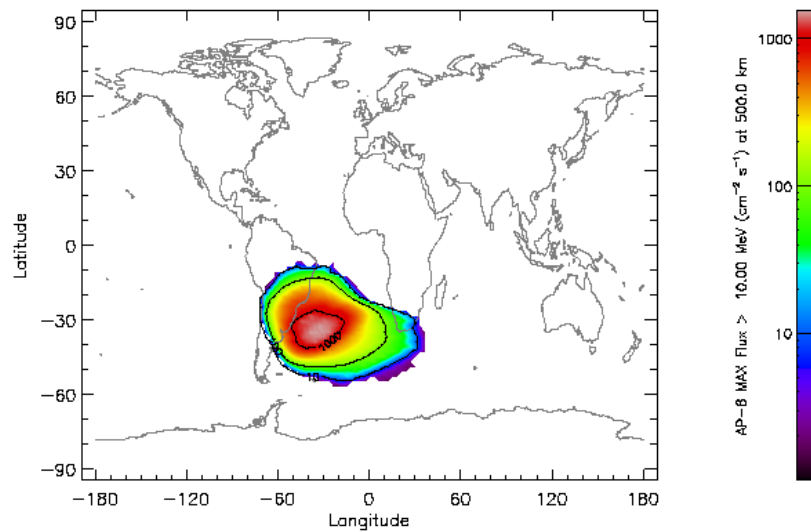


Figure C.3 Map of the proton flux 500 km above the Earth's surface for energies larger than 10.0 MeV in the time of a solar maximum. Generated and plotted with SPENVIS by the use of the AP-8 MAX model.

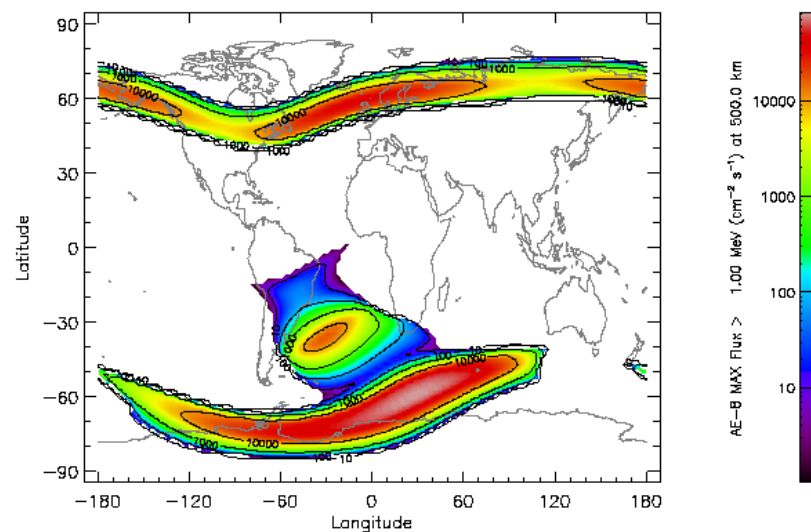


Figure C.4 Map of the electron flux 500 km above the Earth's surface for energies larger than 1.0 MeV in the time of a solar maximum. Generated and plotted with SPENVIS by the use of the AE-8 MAX model.

Possible consequences for satellites passing through the Van Allen belt are that components on the satellite can experience degradation because of ionisation, atomic displacements in the material, and Single Event Upsets (SEU). The impact of these effects depends on the energy of the radiation and the flux that the satellite experiences in its orbit.

The main findings from the simulations reported in [6] related to LEO orbits are that the LEO orbit is lower than the inner Van Allen belt and experiences a low flux for low energy electrons and protons compared to the HEO orbits. It is of interest to note that the LEO orbit, which for most of the cases experiences less electron and proton flux than the other orbits studied (HEO and Medium Earth Orbit), has a very small fall-off in the proton flux for higher energy. This results in the largest flux for proton energies above 100.0 MeV when comparing the various orbits, even though the flux is very small ($\approx 50 \text{ cm}^{-2}\text{s}^{-1}$). This is because the LEO orbit, with its low altitude, passes through the South Atlantic Anomaly, which results in an accumulation of high energy protons, see Figure C.5.

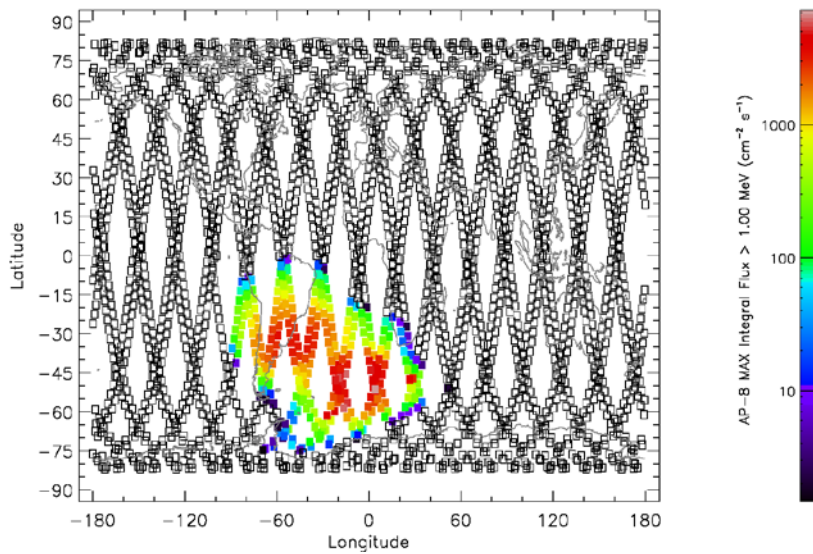


Figure C.5 Proton flux map for energies above 1.0 MeV for the LEO orbit. The large flux concentration is due to the South Atlantic Anomaly. Generated and plotted with SPENVIS.

References

- [1] Lars Erling Bråten, Andreas Nordmo Skauen and Abdikerim Yusuf, “Microsatellites in elliptical orbits for satellite communications,” FFI-Report 16/01896, Kjeller 19.12.2016.
- [2] Rogan Shimmin (Ed.), “Small Spacecraft Technology State of the Art,” NASA/TP–2015–216648/REV1, Mission Design Division, Ames Research Center, Moffett Field, California, Dec. 2015.
- [3] N. Chahat, J. Sauder, R. Hodges, M. Thomson, Y. R. Samii and E. Peral, “Ka-band High-Gain Mesh Deployable Reflector Antenna Enabling the first Radar in a CubeSat: RainCube,” In Proc. 10th European Conference on Antennas and Propagation (EuCAP 2016), Davos, Switzerland, 10-16 April 2016.
- [4] J. G. Walker, “Coverage Predictions and Selection Criteria for Satellite Constellations,” Technical Report 82116, Royal Aircraft Establishment, Dec. 1982.
- [5] T. Tjelta, M. Rytir, L. E. Bråten, P. A. Grotthing, M. Cheffena, J. E. Håkegård “Results of a Ka Band Campaign for the Characterisation of Propagation Conditions for SatCom Systems at High Latitudes,” In Proc. 11th European Conference on Antennas and Propagation (EuCap), Paris, 19 – 24 March 2017.
- [6] K. Bjørke and L. E. Bråten,” Simulations of space weather for communication satellites – a study of highly elliptical and circular orbits,” FFI-rapport 2015/00863.
- [7] <https://www.spennis.oma.be/help/background/traprad/traprad.html>, 2013.
- [8] K. Devaraj, et al., “Dove High Speed Downlink System,” In Proc. AIAA/USU Conference on Small Satellites, Logan, USA, 5-10 Aug., 2017.
- [9] Johan Wettergren, Patrik Dimming, Joakim F. Johansson and Mikael Öhgren, “A high gain X-band isoflux helix antenna,” In Proc. *10th European Conference on Antennas and Propagation (EuCAP)*, 2016.
- [10] Alberto Reyna Maldonado, Marco A. Panduro, Carlos Del Río and Aldo Mendez, “Design of Concentric Ring Antenna Array for a Reconfigurable Isoflux Pattern,”
- [11] Eric Arnaud, Cyrille Menudier, J Fouany, T Monediere and M Thevenot, “X-band compact dual circularly polarized isofux antenna for nanosatellite applications,” *International journal of microwave and wireless technologies*, 2017, pp.1 - 8.
- [12] J. Fouany, et al., “Circularly polarized isoflux compact X band antenna for nanosatellites applications,” In Proc. *12th European Radar Conference*, 2015.
- [13] Y. Kobayashi and S. Kawasaki, “X-band, 15-W-class, highly efficient deep-space GaN SSPA for PROCYON mission,” *IEEE Transactions on Aerospace and Electronic Systems*, vol. 52, issue 3, June 2016.
- [14] H. Noto, et. al., ”X- and Ku-band internally matched GaN amplifiers with more than 100W output power,” In Proc. 42nd European Microwave Conference (EuMC), Amsterdam, Oct. 29 – 1. Nov., 2012.
- [15] W. Boger, D. Burgess, R. Honda and C. Nuckolls, “X-band, 17 Watt, solid-state power amplifier for space applications,” *IEEE MTT-S International Microwave Symposium Digest*, 12-17 June, 2005.

-
- [16] Hirobumi Saito, et al., "High Bit-rate Communication in X Band for Small Earth Observation Satellites - Result of 505 Mbps Demonstration and Plan for 2 Gbps Link," In Proc. Small Satellite Conference, Utah, August 6-11, 2016.
- [17] Daniele Cavallo, et al., "Ku Band Hemispherical Fully Electronic Antenna for Aircraft in Flight Entertainment," In Proc. *IEEE International Symposium on Antennas and Propagation*, 2012.
- [18] V. Arneson, L. Bråten, J. Sander, T. M. O. Mjelde and Ø. Olsen, "Land-mobile X-band Satellite Measurements in Norway, Experiment Description and First Results," In Proc. 11th European Conference on Antennas and Propagation (EUCAP), Paris, 19-24 March 2017.
- [19] "Propagation data and prediction methods required for the design of Earth-space telecommunication systems," ITU-R, Rec. P.618-12, Geneva, 2015.
- [20] Gomspace. (2017) [www.gomspace.com](http://www.gomspace.com/Shop/subsystems/solar-panels/default.aspx). [Online]. <http://www.gomspace.com/Shop/subsystems/solar-panels/default.aspx>
- [21] Gomspace. (2017) [www.gomspace.com](http://www.gomspace.com/Shop/subsystems/batteries/default.aspx). [Online]. <http://www.gomspace.com/Shop/subsystems/batteries/default.aspx>
- [22] Clydespace. (2017) www.clydespace.com [Online.] <https://www.clyde.space/products/47-cs-high-power-bundle-c-eps-80whr-battery>
- [23] Chia-Chun "George" Chao, *Applied Orbit Perturbation and Maintenance*, The Aerospace Corporation, 2005. ISBN 1-884989-17-9.
- [24] Vladimir. A Chobotov, *Orbital Mechanics*, 3rd ed.: American Institute of Aeronautics and Astronautics, Inc., 2002. ISBN 1-56347-537-5.
- [25] David A. Vallado, *Fundamentals of Astrodynamics and Applications*.: McGraw-Hill, 1997. ISBN 0-07-066834-5.
- [26] Jim Franconeri, "Use of Differential Drag as a Satellite Constellation Stationkeeping Strategy", 2003. http://ccar.colorado.edu/asen5050/projects/projects_2003/franconeri/
- [27] J. R. Wertz, "Orbit & Constellation Design & Management," Microcosm, 2009. ISBN 978-0-7923-7148-9.
- [28] Spaceflight Industries, Inc. (2016) www.spaceflight.com. [Online]. Available: <http://www.spaceflight.com/schedule-pricing/>
- [29] Rocket Lab USA. (2017, August) www.rocketlabusa.com. Website. [Online]. <https://www.rocketlabusa.com/latest/rocket-lab-completes-post-flight-analysis/>
- [30] Small Sat launcher. (2016) <http://www.small-launcher.eu/>. [Online]. Available: <http://www.small-launcher.eu/>
- [31] W. K. Tobiska and N. Sarzi-Amade, "Radiation Belts," in *Space Mission Engineering: The New SMAD*, 28 ed. J. R. Wertz, D. F. Everett, and J. J. Puschell, Eds. Microcosm Press, 2011, pp. 134-137.
- [32] N. R. Rigozo, M. P. Souza Echer, H. Evangelista, D. J. R. Nordemann, and E. Echer, "Prediction of sunspot number amplitude and solar cycle length for cycles 24 and 25," in *Journal of Atmospheric and Solar-Terrestrial Physics*, 73 ed. 2010, pp. 1294-1299.
- [33] J. Javaraiah, "Long-term variations in the north-south asymmetry of solar activity and solar cycle prediction, III: Prediction for the amplitude of solar cycle 25," in *New Astronomy*, 34 ed. 2014, pp. 54-64.
- [34] SPENVIS, "Trapped particle radiation models,"

-
-
- [35] Nicholas Crisp, "A Methodology for the Integrated Design of Small Satellite Constellation Deployment," University of Manchester, PhD Thesis 2016.
- [36] VACCO Industries. (2017, August) AFRL Propulsion Unit for Cubesats (PUC). [Online]. <http://www.cubesat-propulsion.com/propulsion-unit/>
- [37] Busek Co. Inc. (2017, August) BET-1mN Busek Electro Spray Thruster. [Online]. http://www.busek.com/index_htm_files/70008500%20BET-1mN%20Data%20Sheet%20RevH.pdf
- [38] Khary I. Parker, "State-of-the-Art for Small Satellite Propulsion Systems," in *2016 NSBE Aerospace Systems Conference*, Arlington, VA, 2016. [Online]. <https://ntrs.nasa.gov/search.jsp?R=20160010585>
- [39] Moog Inc. (2017, August) www.csaengineering.com. [Online]. <http://www.csaengineering.com/products-services/espa/>
- [40] Jordi Puig-Suari and Guy Zohar, "Deployment of CubeSat Constellations Utilizing Current Launch Opportunities," in *27th Annual AIAA/USU Conference on Small Satellites*, Logan, Utah, 2013.

About FFI

The Norwegian Defence Research Establishment (FFI) was founded 11th of April 1946. It is organised as an administrative agency subordinate to the Ministry of Defence.

FFI's MISSION

FFI is the prime institution responsible for defence related research in Norway. Its principal mission is to carry out research and development to meet the requirements of the Armed Forces. FFI has the role of chief adviser to the political and military leadership. In particular, the institute shall focus on aspects of the development in science and technology that can influence our security policy or defence planning.

FFI's VISION

FFI turns knowledge and ideas into an efficient defence.

FFI's CHARACTERISTICS

Creative, daring, broad-minded and responsible.

Om FFI

Forsvarets forskningsinstitutt ble etablert 11. april 1946. Instituttet er organisert som et forvaltningsorgan med særskilte fullmakter underlagt Forsvarsdepartementet.

FFIs FORMÅL

Forsvarets forskningsinstitutt er Forsvarets sentrale forskningsinstitusjon og har som formål å drive forskning og utvikling for Forsvarets behov. Videre er FFI rådgiver overfor Forsvarets strategiske ledelse. Spesielt skal instituttet følge opp trekk ved vitenskapelig og militærteknisk utvikling som kan påvirke forutsetningene for sikkerhetspolitikken eller forsvarsplanleggingen.

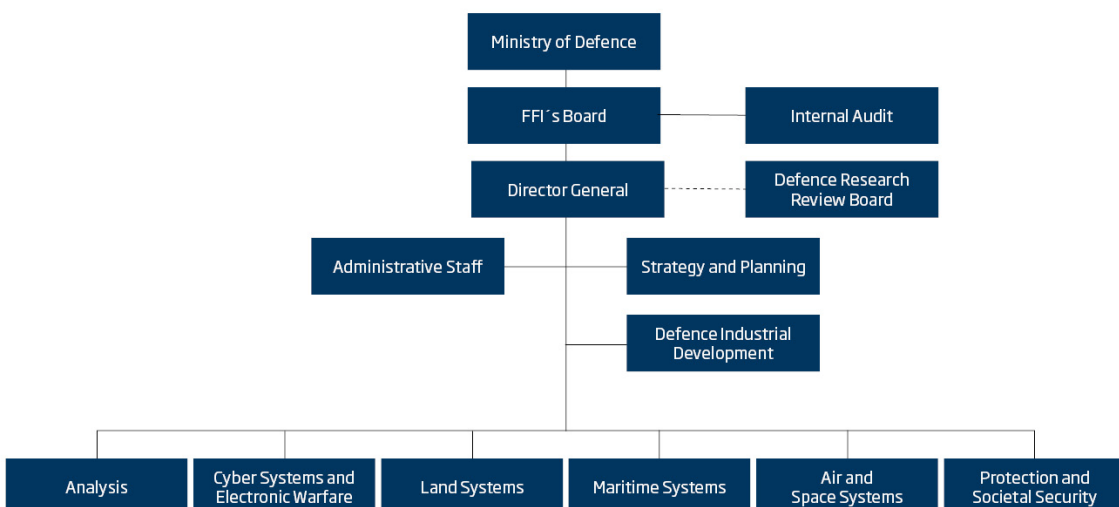
FFIs VISJON

FFI gjør kunnskap og ideer til et effektivt forsvar.

FFIs VERDIER

Skapende, drivende, vidsynt og ansvarlig.

FFI's organisation



Forsvarets forskningsinstitutt
Postboks 25
2027 Kjeller

Besøksadresse:
Instituttveien 20
2007 Kjeller

Telefon: 63 80 70 00
Telefaks: 63 80 71 15
Epost: ffi@ffi.no

Norwegian Defence Research Establishment (FFI)
P.O. Box 25
NO-2027 Kjeller

Office address:
Instituttveien 20
N-2007 Kjeller

Telephone: +47 63 80 70 00
Telefax: +47 63 80 71 15
Email: ffi@ffi.no